The Mycobactin Biosynthesis Pathway: A Prospective Therapeutic Target In The Battle Against Tuberculosis

Mousumi Shyam[1,3], Deepak Shilkar[1], Harshita Verma[3], Abhimanyu Dev[1], Barij Nayan Sinha[1], Federico Brucoli[2]*, Sanjib Bhakta[3]*, Venkatesan Jayaprakash[1]*

[1]*Department of Pharmaceutical Sciences & Technology, Birla Institute of Technology, Mesra, Ranchi 835215 (JH), India*

[2]*Leicester School of Pharmacy, De Montfort University, The Gateway, Leicester LE1 9BH, UK*

[3]*Mycobacteria Research Laboratory, Department of Biological Sciences, Institute of Structural and Molecular Biology, Birkbeck, University of London, Malet Street, London WC1E 7HX, UK*

*Corresponding authors.

E-mail: drvenkatesanj@gmail.com (V. Jayaprakash)

E-mail: s.bhakta@bbk.ac.uk/ sanjib.bhakta@ucl.ac.uk (S. Bhakta)

E-mail: federico.brucoli@dmu.ac.uk (F. Brucoli)

ABSTRACT: The alarming rise in drug-resistant clinical cases of tuberculosis (TB) has necessitated the rapid development of newer chemotherapeutic agents with novel mechanisms of action. The mycobactin biosynthesis pathway, conserved only among the mycolata family of actinobacteria, a group of intracellularly surviving bacterial pathogens that includes *Mycobacterium tuberculosis,* generates a salicyl-capped peptide mycobactin under iron-stress conditions in host macrophages to support the iron demands of the pathogen. This *in vivo* essentiality makes this less explored mycobactin biosynthesis pathway a promising endogenous target for novel lead-compounds discovery. In this perspective, we have provided

an up-to-date account of drug discovery efforts targeting selected enzymes (MbtI, MbtA, MbtM, and PPTase) from the *mbt* gene cluster (*mbtA-mbtN*). Furthermore, a succint discussion on nonspecific mycobactin biosynthesis inhibitors and the Trojan horse approach adopted to impair iron metabolism in mycobacteria has also been included in this review.

Keywords

Mycobactin; mycobacterial siderophore; antitubercular agents; target validation; conditionally essential targets; salicyl-AMP analogs

1. Introduction:

I. Clinically approved antitubercular chemotherapeutics and their evolving drug resistance mechanism:

TB is an ancient infectious disease caused by the deadly pathogen *Mycobacterium tuberculosis* (Mtb).[1, 2] This bacterium has plagued humanity for centuries and is now the cause of a global pandemic.[3,4] According to the 2020 World Health Organization (WHO) report, TB was responsible for about 1.4 million deaths, and over 10 million fell ill with TB worldwide in 2019, implying its dreadful impact on the global mortality and morbidity rate.[5] The WHO estimates that about one in four individuals has an established TB infection as of date.[6] Other *Mycobacterium* genus members, such as *Mycobacterium bovis* and *Mycobacterium africanum*, are also cumulatively affecting the world population.[7] TB is an airborne disease, and as most of the infections of this kind, do not reach the active phase immediately after reaching the target. Due to its ability to adapt to the human immune system, Mtb survives latently infected individuals in a non-replicating or dormancy-like state for an indefinite period, reactivating only when there is an immune imbalance.[8] Bacillus resistance during the latent phase is

accomplished by producing reactive nitrogen intermediates (RNIs), e.g., NO, NO_2, and N_2O_3, blockade of phagosome-lysosome fusion, and interference with MHC class II antigen.[9] Activation of the resuscitation promotion factors,[10,11] i.e., Rpf A to E. Rpf (peptidoglycan-hydrolyzing enzymes), enables Mtb to re-enter the active phase whereas Mtb DosR regulon system, *dosR* (Rv3133c),[12,13] enables a transition from respiring to non-respiring conditions and vice versa without loss of viability, jointly leading to active and contagious tuberculosis infection.[14] These salient features of the bacilli make TB one of the most challenging infectious diseases to combat and eradicate.[15,16] The golden era of TB antibiotic discovery commenced with the *p*-aminosalicylic acid development in 1943, followed by the discovery of streptomycin as the first antitubercular agent in 1944.[17,18,19] This was followed by a series of antitubercular drug discoveries, including isoniazid and pyrazinamide in 1952, ethambutol in 1961, and rifampicin in 1963, with the latter remaining as the keystone for anti-TB therapy to date.[20,21,22,23,24] (**Figure 1**)

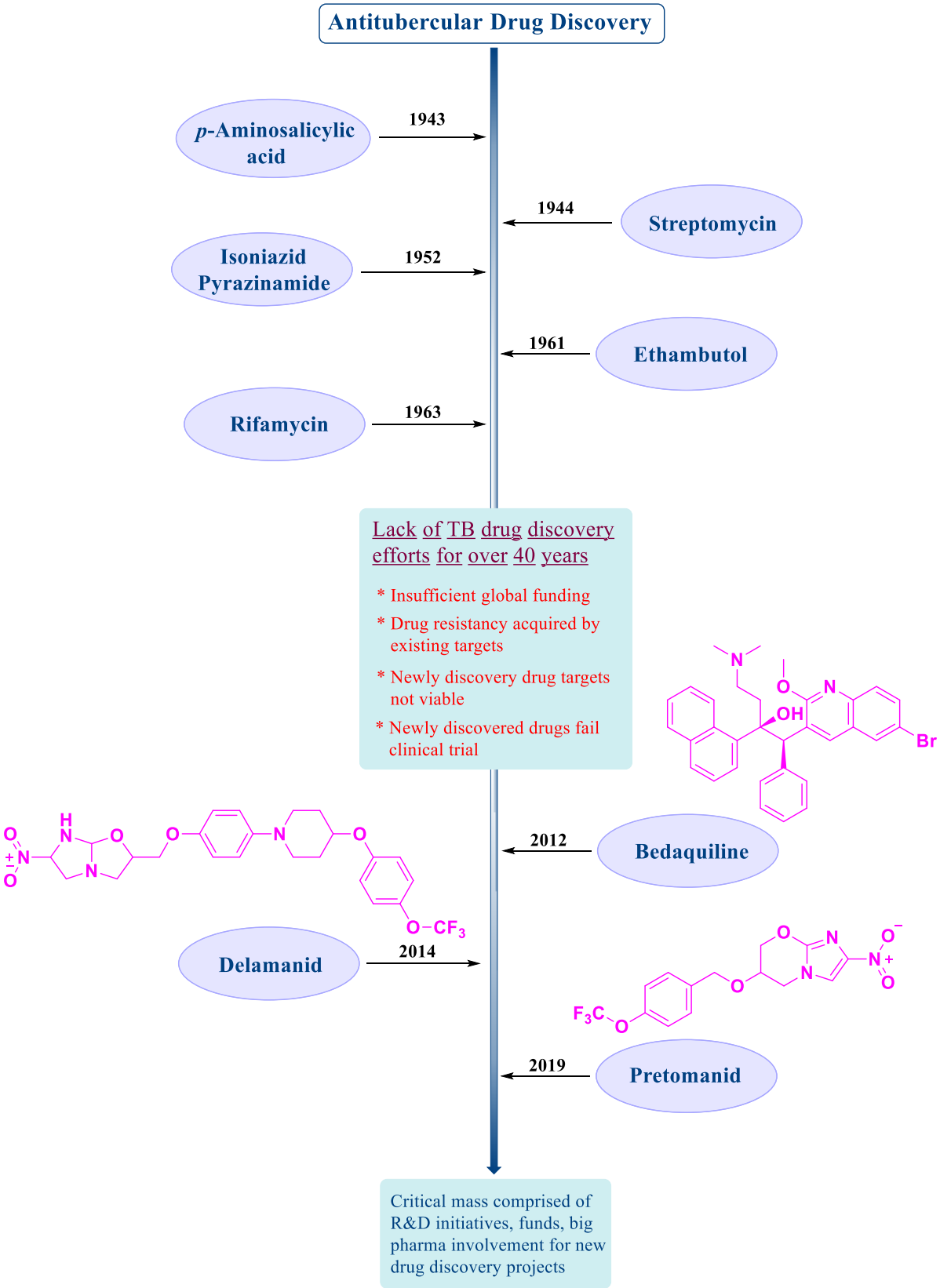
Antitubercular Drug Discovery
p-Aminosalicylic acid
1943
1944
Streptomycin
Isoniazid
Pyrazinamide
1952
1961
Ethambutol
Rifamycin
1963
Lack of TB drug discovery efforts for over 40 years
* Insufficient global funding
* Drug resistancy acquired by existing targets
* Newly discovery drug targets not viable
* Newly discovered drugs fail clinical trial
2012
Bedaquiline
Delamanid
2014
2019
Pretomanid
Critical mass comprised of R&D initiatives, funds, big pharma involvement for new drug discovery projects

Figure 1. A schematic description of the chronological discovery sequence of clinically approved antitubercular drug candidates. Starting with the *p*-aminosalicylic acid and moving to the recently approved pretomanid, indicating the progress in TB management over 76 years.

In the mid-1980s, a significant resurgence of TB infections occurred primarily due to the prevalence of extensively drug-resistant (XDR) or multi-drug-resistant (MDR) strains, which were potentially incurable with available therapies.[25] In 1993, the WHO declared TB a global health emergency to draw the world's attention to the growing severity of the TB epidemic.[26] Due to the continuous evolution of essential genetic material and the rapid propagation of drug-resistant tuberculosis pathogens, the therapeutic efficacy of the drugs reduced drastically over time. Moreover, the lack of investment in R&D from big pharmaceutical companies in newer candidates' discoveries worsened over the last few decades. Clinical approval of new drugs, i.e., bedaquiline (2012),[27,28,29] delamanid (2014),[30,31] and pretomanid (2019)[32,33] came more than four decades after the discovery of rifampicin (more information is summarized on the following website; https://www.newtbdrugs.org/pipeline/discovery) (**Figure 1**). Like first-line TB drugs, the newly discovered drugs also targeted the products of essential genes (essential for the sustenance of the microorganism in any environment).[34] Although bedaquiline, delamanid, and pretomanid remain the only solution against drug resistance-TB to date, the slow emergence of drug-resistant cases to these new drugs forecasts a grim scenario in antitubercular chemotherapy. This also highlights the need for newer chemical entities with novel modes of action to mitigate the emerging burden of MDR, XDR, and totally drug-resistant (TDR)-TB.[35,36,37]

We have summarized the established essential drug targets and the mechanism underlying the development of drug resistance for each target in **Table 1**. We believe that this

will encourage medicinal chemists to search for alternative drug targets and investigate newer ways of tackling drug resistance.

Table. 1. A summary of drugs, targets, and common resistance mechanisms for clinically approved antitubercular agents

Drug	**Discovery/ Approval**	**Target**	**Resistance Mechanism**
p-aminosalicylic acid (PAS)	1943	The mechanism of action of PAS remains elusive, although it is thought that this drug might act as an antimetabolite of salicylic acid and be involved in some steps of the metabolic pathway of iron uptake.[38] More recently, PAS mode of action has been linked to the disruption of folate metabolism in Mtb, as this prodrug was found to target dihydrofolate reductase (DHFR) and modulate	Mutation in the *thyA* gene in addition to *folC* and *ribD* genes, has been identified as the leading reason behind PAS resistance.[40,41]

		thymidylate synthase (*thyA*) activity.[39]	
Streptomycin	1944	Inhibits protein synthesis by targeting S12 protein and 16S rRNA components of the 30S ribosomal subunit.[42]	Mutation at 30S ribosomal protein S12 (rpsL) and 16S ribosomal RNA (rrs) genes conferring binding site modulation.[43]
Isoniazid	1952	Inhibits cell wall mycolic acid biosynthesis by targeting NADH-dependent enoyl acyl carrier protein reductase.[44]	Suppression of catalase-peroxidase (KatG) enzymes responsible for prodrug activation of INH result in a decrease of the active drug release, and mutation of inhibin Subunit Alpha (inhA) gene causes overexpression of inhA protein.[45]
Pyrazinamide	1952	Inhibits membrane energetics and phthiocerol dimycocerosates (PDIM) synthesis by interfering with aspartate decarboxylase (PanD), Mycocerosic acid synthase,	Mutations in pyrazinamidase/nicotinamidase (pncA) gene reduce the conversion of pyrazinamide to active pyrazinoic acid form.[47]

		and phenolthiocerol synthesis type-I polyketide synthases.[46]	
Ethambutol	1961	Inhibits cell wall arabinogalactan synthesis by targeting Arabinosyl transferase enzyme.[48]	Mutation at arabinosyl transferase (embB306) codon of embB gene responsible for the synthesis of a critical structural component of the mycobacterial cell wall, arabinogalactan, and lipoarabinomannan.[49]
Rifampicin	1963	Inhibits RNA synthesis by the β subunit of RNA polymerase.[50]	Mutation at the subunit of RNA polymerase (rpoB) gene causes conformational changes.[51]
Bedaquiline	2012	Inhibition of mitochondrial ATP synthase.[52,53]	Mutation at the *atpE* gene and Rv0678 conferring drug resistance. *atpE* gene encodes the trans membrane oligomeric C subunit of ATP synthase, preventing the drug from binding at the C subunit. Whereas Rv0678 is a transcriptional repressor

			encoding the MmpS5-MmmpL5 efflux pump involves in resistance to bedaquiline.[54]
Delamanid	2014	Inhibits Methoxymycolic acid and ketomycolic acid biosynthesis.[55]	Mutation of the five genes *ddn*, and *fgd1*, *fbiA*, *fbiB*, *fbiC* genes associated with either prodrug activation or F_{420} biosynthetic pathway have been identified as the reason of drug resistance.[56,57]
Pretomanid	2019	Targeting the cell wall biosynthesis inhibition and causing respiratory poisoning through nitric oxide (NO) release.[58] Additionally by targeting the pentose phosphate pathway results in the accumulation of lethal methylglyoxal.[59]	Function mutation in *ddn*, *fgd1*, *fbiA*, *fbiB*, and *fbiC* causes drug resistance.[56,57]

II. Conditionally Essential Target, Mycobactin, and its role as a significant drug platform for drug-resistant TB:

There is an urgent need for new antitubercular agents, which act via novel mechanisms different from the presently available drugs. This can be achieved using the concept of "Conditionally Essential Target (CET)" based drug design. A good example of a conditionally essential process in *mycobacteria* would be the acquisition of iron, an essential nutrient for bacterial biochemical machinery,[60,61,62] from the human host reservoirs. The concentration of iron in our serum or body fluids is significantly low (approx. 10^{-24} M) to support bacterial colonization and growth.[63] The extracellular iron in the host body is primarily bound to various iron transport proteins, such as transferrin and lactoferrins, and the intracellular iron is sequestered by the 'heme' group stored within the iron-sulfur cluster of the storage protein ferritin.[64,65] Mycobacteria have evolved several mechanisms to acquire iron when faced by scarcity within the host. The most prominent is the synthesis, secretion, and reuptake of small molecules termed mycobactins (mycobacterial siderophores or iron chelators).[66,67,68] Mycobacteria acquire iron from their host cell through the mycobactin-mediated iron transportation system. This siderophore biochemical machinery is up-regulated when Mtb face iron-deficient conditions, as experienced by Mtb in macrophages, and is one of the major pathogenic determinants of TB.[69,70]

Mycobactins are hexadentate ligands with a tripodal architecture. Their basic scaffold consists of an ortho-hydroxy phenyl - oxazoline system attached to an acylated hydroxylysine residue esterified with a 3-hydroxybutyric acid unit. This linker is, in turn, tethered to a terminal cyclized hydroxylysine moiety forming a seven-membered lactam ring. Mycobactins exhibit a very high affinity toward the ferric ion Fe (III) as they form a stable binary complex, with a stability constant (K_s) of ~10^{-25} (**Figure 2**).[71,72,73,74,75] Mtb produces two main types of siderophores, e.g., carboxymycobactin and mycobactin T. The hydrophilic carboxymycobactin

(a highly soluble peptide molecule)[76,77,78] is normally released in the extracellular space. It chelates and internalizes iron as a ferri-carboxymycobactin complex at physiological pH (2–8) and transfers Fe (III) to the more lipophilic mycobactin-T[79] that is associated with the mycobacterial cell wall. Another class of siderophores, termed exochelins, are produced by saprophytic mycobacteria, such as *Mycobacterium smegmatis* (*Msmeg*)[80] or *Mycobacterium neoaurum* (*Mneo*).[81] Unlike carboxymycobactin and mycobactin (virulence factors), these are considered avirulent factors that indicate ongoing TB infections. Exochelin is a peptide-based, highly water-soluble molecule, and its hydrophilic nature facilitates sequestration of Fe (III) from the aqueous-aerobic environment of the host tissues followed by release into the intracellular environment, where it is taken up by membrane-bound lipophilic mycobactins. A study conducted on the exochelin-*Msmeg* scaffold indicates that the presence of 3-hydroxamic acid group on the highly charged formylated pentapeptide backbone is responsible for Fe (III) chelation and formation of ferri-exochelin complex at physiological pH 5–6.8 from transferrin and ferritin.[82] (**Figure 2**)

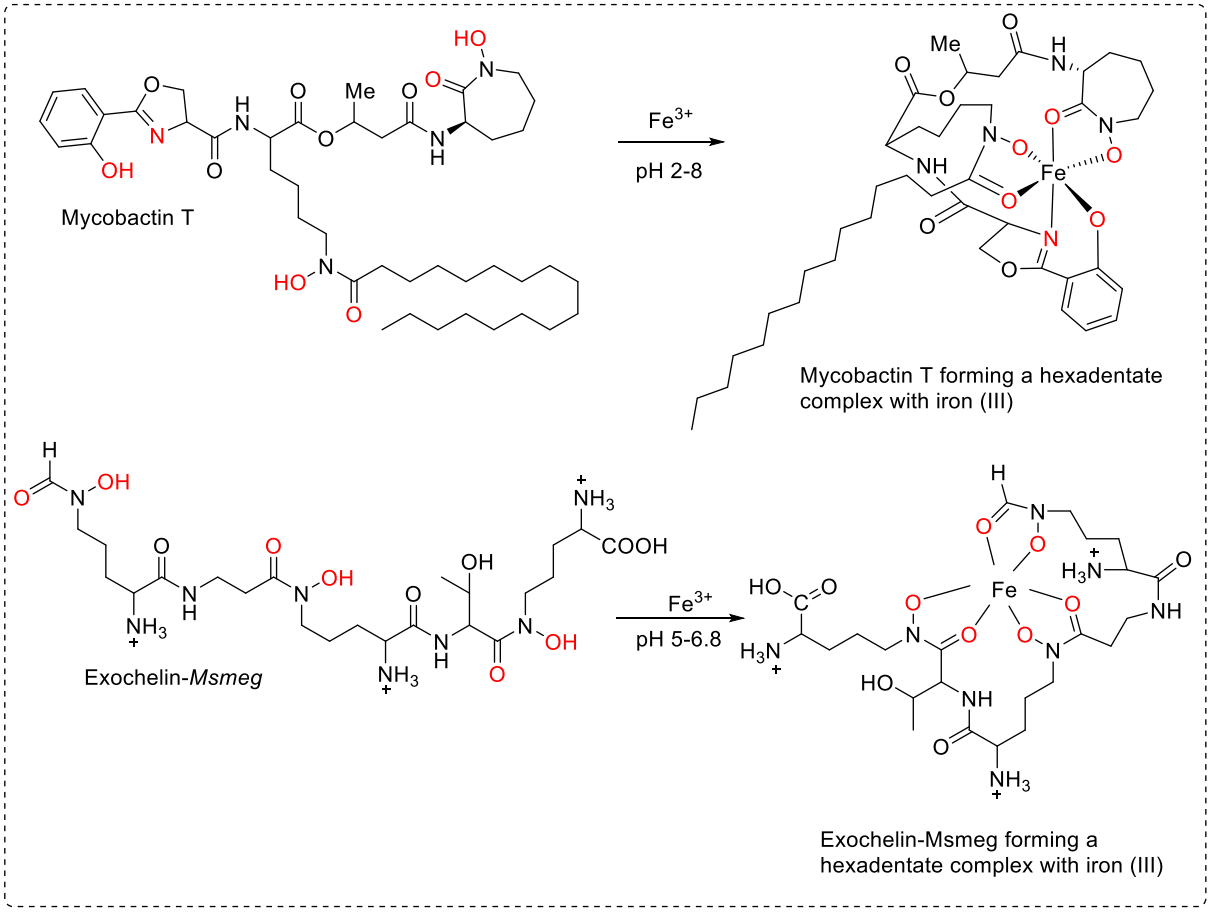

Figure 2. Mycobactin T and Exochelin-*Msmeg* forming a hexadentate complex with iron (III) within a pH range of 2–8 and 5–6.8, respectively.

Ferri-carboxymycobactin uptake occurs through a porin transport system, involving a facilitated diffusion process. Excess iron is transferred to the intra-envelope storage of iron, mycobactin. The ferri-reductase enzyme present at the intracellular membrane releases the Fe (II) from ferri-carboxymycobactin in the cytoplasm. Fe (II) forms a complex with salicylate residues and is transported to the mycobacterial iron storage apoprotein – bacterioferritin.[83,84,85] (**Figure 3**) A study performed by Rodriguez and Smith[86] using the irtAB mutant strain in C57B/6 mice model and THP1-macrophage cell line indicates that irtAB gene mutant strains were unable to utilize ferri-carboxymycobactin efficiently. They further postulated that the IrtAB might be a transporter of Fe-carboxymycobactin and that the iron transportation process may be regulated by the IdeR transcription factor. They concluded that preventing the Fe-

carboxymycobactin uptake mechanism can hinder the survival of *mycobacteria* under iron-deficient conditions.

In the case of *Msmeg*, upon being recognized by the cell surface receptor protein (Rec) and, after that, via FxuD conjunction, the ferri-exochelin complex penetrates the membrane through the FxuA, FxuB, and FxuC system. The reductase enzyme present in the cytoplasm releases Fe (II) at the expenses of ATP. Bacterioferritin present in the cytoplasm is responsible for the storage of Fe (II). In case of Rec and FxuABC transport system unavailability, the sequestration of Fe (II) from ferri-exochelin is carried out by mycobactin without energy input.[87,88] (**Figure 3**)

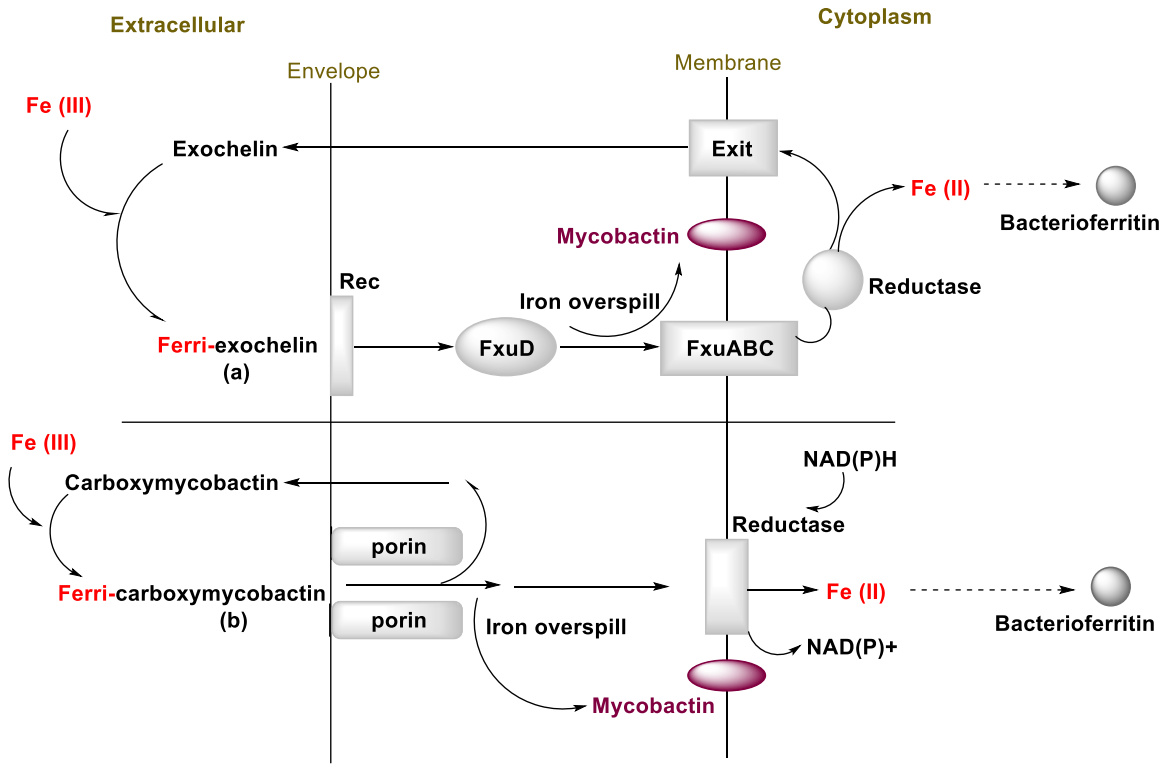

Figure 3. General diagrammatic representation of the different possible modes of iron uptake mechanism involving exochelin, mycobactin, and carboxymycobactin in mycobacteria. (a). Non-membrane-associated exochelins form a stable ferri-exochelin complex recognized by the surface receptor protein (Rec) that allows the complex to be taken across the cell envelope. Membrane penetration of the ferri-exochelin complex occurs through

the FxuA, FxuB, and FxuC systems. Reductase enzymes present in the cytoplasm release Fe (II) ions, which are then incorporated into mycobacterial apoproteins, such as bacterioferritin (Bfr). **(b).** The ferri-carboxymycobactin uptake is facilitated by a diffusion mechanism through the membrane transport protein, porin. Membrane-associated reductase releases Fe (II) within the cytoplasm.

The mycobactin biosynthesis pathway has long attracted interest as a viable source of antitubercular targets for the design and development of novel probes. Snow et al.[69] in 1970 first reported the experimental observation illustrating the inhibitory property of mycobactin M and N (isolated from *Mycobacterium marinum*) against *Mycobacterium paratuberculosis* and Mtb (**Figure 4**). This property was mainly attributed to their chemical structure that considerably differs from those of H37Rv mycobactin and carboxymycobactin. This finding prompted many researchers to synthesize analogs of mycobactins to study their ability to promote or inhibit mycobacterial growth.[89] The total synthesis of mycobactin S was achieved in 1983 by Maurer and Miller.[90] Mycobactin S (1997), an analog of mycobactin T (originally isolated by Snow et al. in 1965 from Mtb in their lab), reportedly had a different configuration at the chiral center on the 3-hydroxybutyrate carbon skeleton (**Figure 4**) and was found to inhibit the growth of Mtb by competitive iron chelation. However, Mtb revived due to the enhancement in the production of natural siderophores and their competitive iron chelation mechanism.[91] Poreddy et al.[92] made similar observations in 2003 and adopted a different approach targeting the Mtb iron acquisition pathway by investigating enzymes directly involved in the biosynthesis of mycobactins.[93]

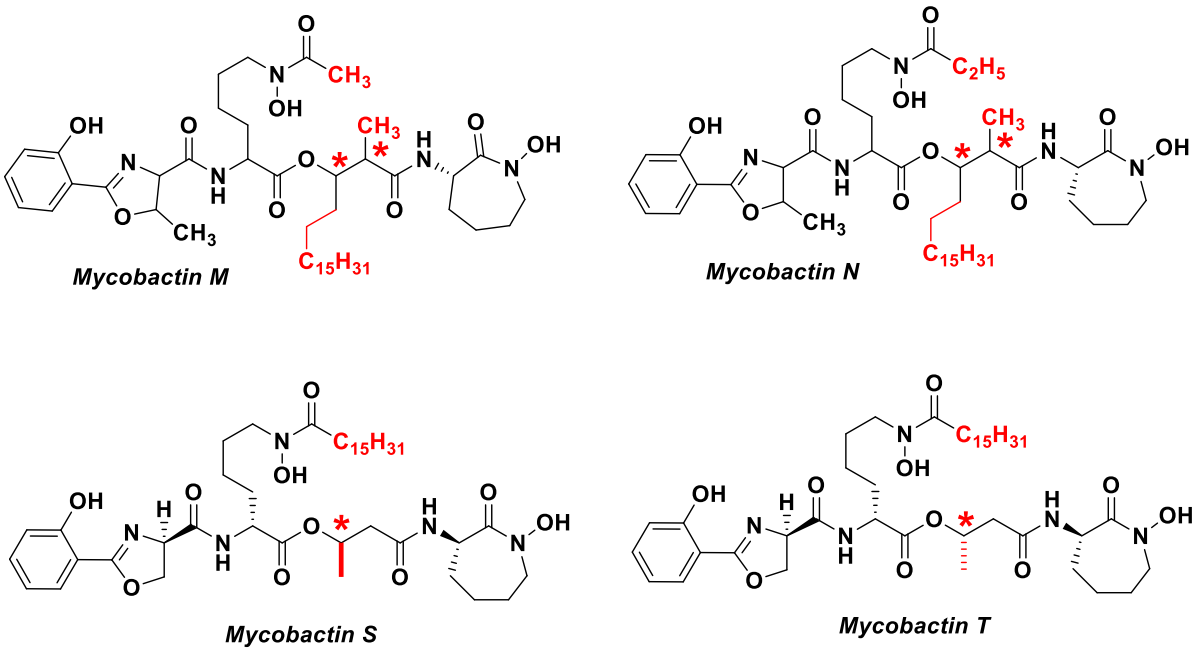

Figure 4. Chemical structure of the different mycobactin analogs, mycobactin M, mycobactin N, mycobactin S, and mycobactin T. Asterisk (*) indicates the chiral center in the respective mycobactin structures.

Mycobactin biosynthesis is carried out by a mixed nonribosomal peptide synthetase-polyketide synthase (NRPS-PKS) hybrid system encoded by 14 essential genes in the *mbt* gene cluster (*mbtA-mbtN*).[69,93,94,95] (**Figure 5**) The *mbt* gene cluster I (*mbtA-mbtJ*)[93] codes for enzymes (MbtA-J), responsible for the synthesis of the heterocyclic scaffold, i.e., 2-hydroxyphenyloxazolidine unit, whereas the addition of terminal aliphatic residue to salicyl-capped moiety is carried out by the MbtK-MbtN enzymes encoded by the *mbt* gene cluster II (*mbtK-mbtN*).[93,96,97] The aromatic shikimate pathway[98,99] generates chorismate from the shikimic acid, which acts as a starter unit for mycobactin biosynthesis. Next, MbtI catalyzes the transformation of chorismate to salicylic acid,[100,101,102] which is activated by the adenylating enzyme MbtA to the salicyl-adenosine monophosphate (Sal-AMP) at the expense of ATP. MbtA is a bifunctional enzyme that loads Sal-AMP onto the thiolation domain of MbtB, an acyl carrier protein, which is also part of the NRPS-PKS cluster. Vergnolle et al. reported that

MbtA function is reversible and post-transnationally regulated by the acetylation mechanism in Protein lysine acetyltransferase (Pat) and deacetyltransferase (DAc) enzymes.[103] Pat acetylates MbtA on residue Lys546, and the acetylation can be reversed by the NAD+ dependent DAc enzyme. The important connection between the Pat/DAc reversible acetylation system and MbtA together play a significant role in Mtb survival at iron-limiting conditions for mycobacterial infection. In the macrophage phagosome model at low pH (pH 6) and iron-limiting condition, ΔPat strains grow significantly faster than the wild type, while ΔDAc grows considerably slower. The study concluded that while acetylation of MbtA or FadD33 is prevented in ΔPat strains, resulting active enzymes can generate the required level of mycobactin for survival in the macrophage model. In contrast, in the ΔDAc strain, MbtA and FadD33 function at less than full potential, resulting in insufficient mycobactin production, which influences the Mtb survival of the macrophage. MbtB and MbtE are responsible for the inclusion of the serine and lysine residues, respectively, into the siderophore framework, followed by the addition of two malonyl CoA residues in the presence of MbtC and MbtD enzymes. The terminal lysine unit is incorporated by MbtF. Further modifications of the lysine residue are catalyzed by MbtK and MbtG, resulting in the development of the entire mycobactin scaffold.[104,105] MbtH plays a pivotal supporting role in the formation of soluble NRPS proteins, including MbtB, MbtE, and MbtF.[95] Additionally, the phosphopantetheinyl transferase (PPTase) enzyme plays a significant role by converting the *apo* carrier protein domains into the holo domains of mycobactin megasynthetase.[93,106] De Voss et al. performed MbtB gene replacement through homologous recombination modeling and with the hygromycin-resistance cassette of Mtb H37Rv, creating a mutant. The mutant strain showed restricted growth in iron-deficient medium but showed normal growth in the iron supplemented medium. Moreover, the mutant failed to grow in the macrophage cell line as well as in THP-1 cells.[107] Chavadi et al.[94] (2011) reported that ΔmbtA, ΔmbtB, ΔmbtC, ΔmbtD, ΔmbtE, ΔmbtF,

ΔmbtG, and ΔmbtT mutant *Msmeg* strains were not able to produce an appreciable amount of mycobactin, indicating the essentiality of Mbt ABCDEFGT NRPS-PKS enzymatic machinery in the biosynthesis of the core scaffold of the mycobactin. Bythrow et al.[108] construct *Msmeg* ΔEM (deficient of both exochelin and mycobactin gene) failed to show growth in an iron-limiting environment (GAS media, pH 6.6). Based on these findings, we can conclude that the absence of the mycobactin gene leads to growth inhibition in iron-deficient condition, thereby indicating the significance of the *mbt* gene. This evidence highlights the significance of the *mbt* gene cluster for survival in iron-deficient conditions.

To date, only four enzymes, i.e., MbtI, MbtA, MbtM, and PPTase, belonging to the mycobactin biosynthesis pathway, have been investigated as potential TB drug targets. This review will focus on the small molecule inhibitors reported so far, active against these four enzymes, e.g., MbtI, MbtA, MbtM, and PPTase. Based on reported inhibitors design and development efforts, a concise SAR discussion has also been provided. Moreover, the possibilities of exploring other enzymes as potential drug targets have also been discussed.[109] A short note on nonspecific small molecule development, targeting mycobactin biosynthesis pathway and non-conventional antitubercular drug delivery approach, i.e., Trojan Horse model in antitubercular drug discovery, has also been added.

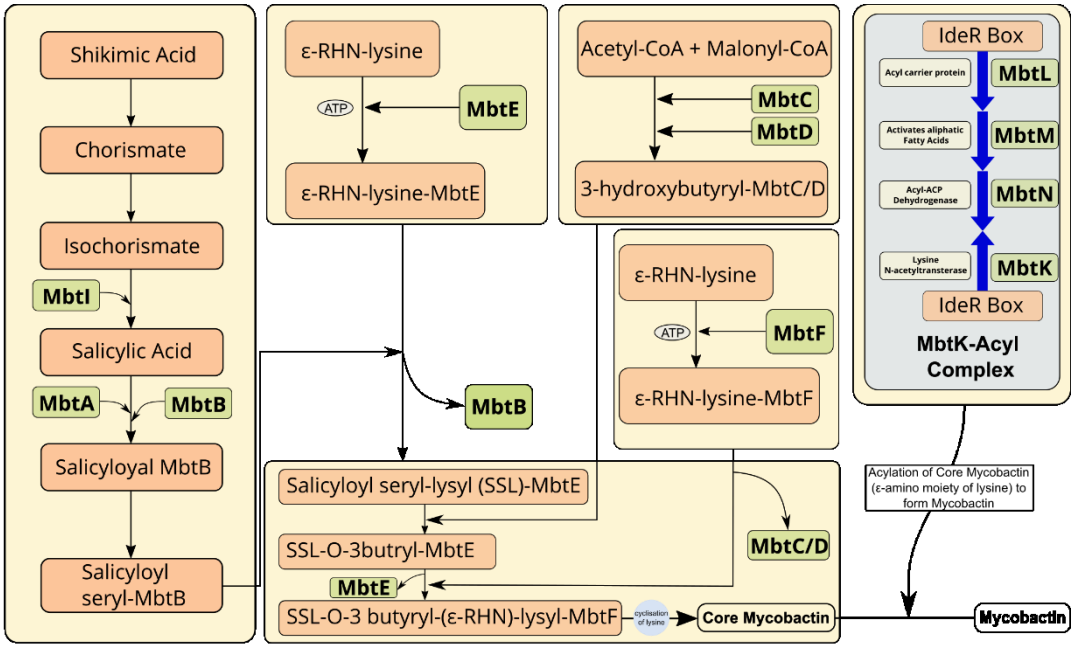
Shikimic Acid
Chorismate
Isochorismate
MbtI
Salicylic Acid
MbtA
MbtB
Salicyloyal MbtB
Salicyloyl seryl-MbtB
ε-RHN-lysine
ATP
MbtE
ε-RHN-lysine-MbtE
Acetyl-CoA + Malonyl-CoA
MbtC
MbtD
3-hydroxybutyryl-MbtC/D
IdeR Box
Acyl carrier protein
MbtL
Activates aliphatic Fatty Acids
MbtM
Acyl-ACP Dehydrogenase
MbtN
Lysine N-acetyltransterase
MbtK
IdeR Box
MbtK-Acyl Complex
ε-RHN-lysine
ATP
MbtF
ε-RHN-lysine-MbtF
MbtB
Salicyloyl seryl-lysyl (SSL)-MbtE
SSL-O-3butryl-MbtE
MbtE
MbtC/D
SSL-O-3 butyryl-(ε-RHN)-lysyl-MbtF
Core Mycobactin
Acylation of Core Mycobactin (ε-amino moiety of lysine) to form Mycobactin
Mycobactin

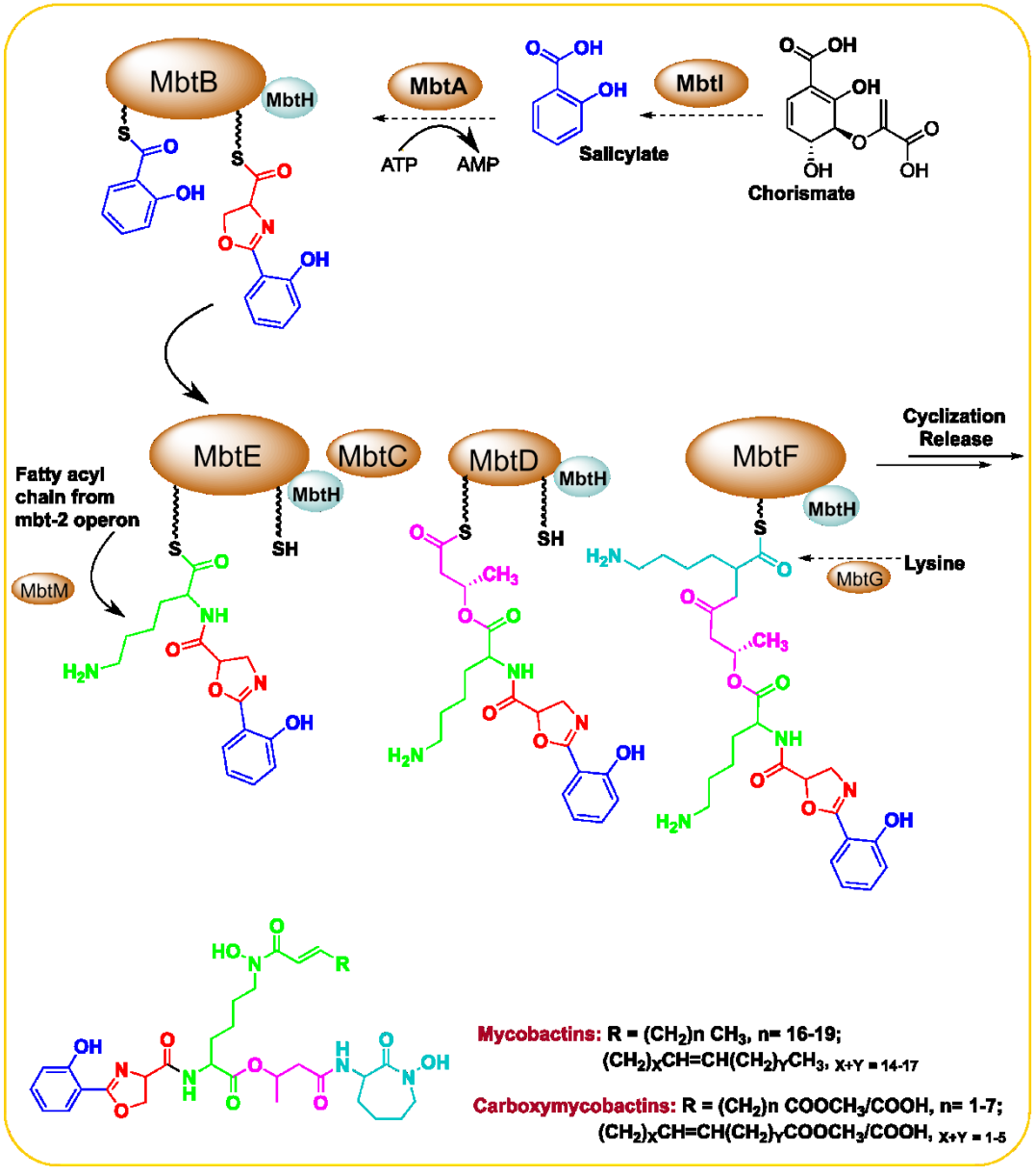
MbtB
MbtH
MbtA
ATP
AMP
Salicylate
MbtI
Chorismate
MbtE
MbtC
MbtD
MbtF
Fatty acyl chain from mbt-2 operon
MbtM
Cyclization Release
Lysine
MbtG
Mycobactins: R = (CH2)n CH3, n= 16-19;
(CH2)XCH=CH(CH2)YCH3, X+Y = 14-17
Carboxymycobactins: R = (CH2)n COOCH3/COOH, n= 1-7;
(CH2)XCH=CH(CH2)YCOOCH3/COOH, X+Y = 1-5

Figure 5. Schematic model of the Mycobactin Biosynthesis Pathway. The biosynthesis pathway involves a complex of nonribosomal peptide synthetase and polyketide synthase (NRPS-PKS) assembly chain. In this pathway, various building blocks, such as salicylate and modified lysine residues, are synthesized by the enzymes outside the assembly chains and covalently tethered to selected domains of the NRPS-PKS enzymes. Amino acids are subsequently added to the growing mycobactin molecule.

3. Drug discovery progress on targeting enzymes involving mycobactin biosynthesis pathway:

*I. Salicylate Synthase (*MbtI*) Inhibitors:*

MbtI is a magnesium (Mg^{2+})-dependent bifunctional salicylate synthase belonging to a large family of chorismate-utilizing enzymes (CUEs). The shikimate pathway plays a vital role in chorismate biosynthesis through the intermediate isochorismate.[102,110] MbtI catalyzes the conversion of chorismate to salicylate, which is further employed in the mycobactin assembly process. Apart from MbtI, other enzymes belonging to the CUEs family, such as 4-amino-4-deoxychorismate synthase (ADCS) and anthranilate synthase (AS), catalyze the production of folate and tryptophan, respectively. In addition to this, isochorismate synthase catalyzes the synthesis of both enterobactin and menaquinone.[111,112,113] Here, we have focused on MbtI due to its significance in salicylate production, which is the starting point of the mycobactin synthesis. Inhibition at this step effectively reduces the pathogenicity of Mtb in the iron-stress condition, without causing toxicity to the host, due to the absence of this enzyme (MbtI or its homologs) in the host cells. MbtI inhibitors are divided into two major classes based on chemical modifications, *i.e.,* transition state (TS) analogs (**Figure 6 & 7**) and non-transition state (Non-TS) analogs (**Figure 8**). The core structure of a TS analog comprises a framework

of chorismate, whereas non-TS analogs are small heterocyclic scaffolds-based inhibitors. These are discussed below in further detail.

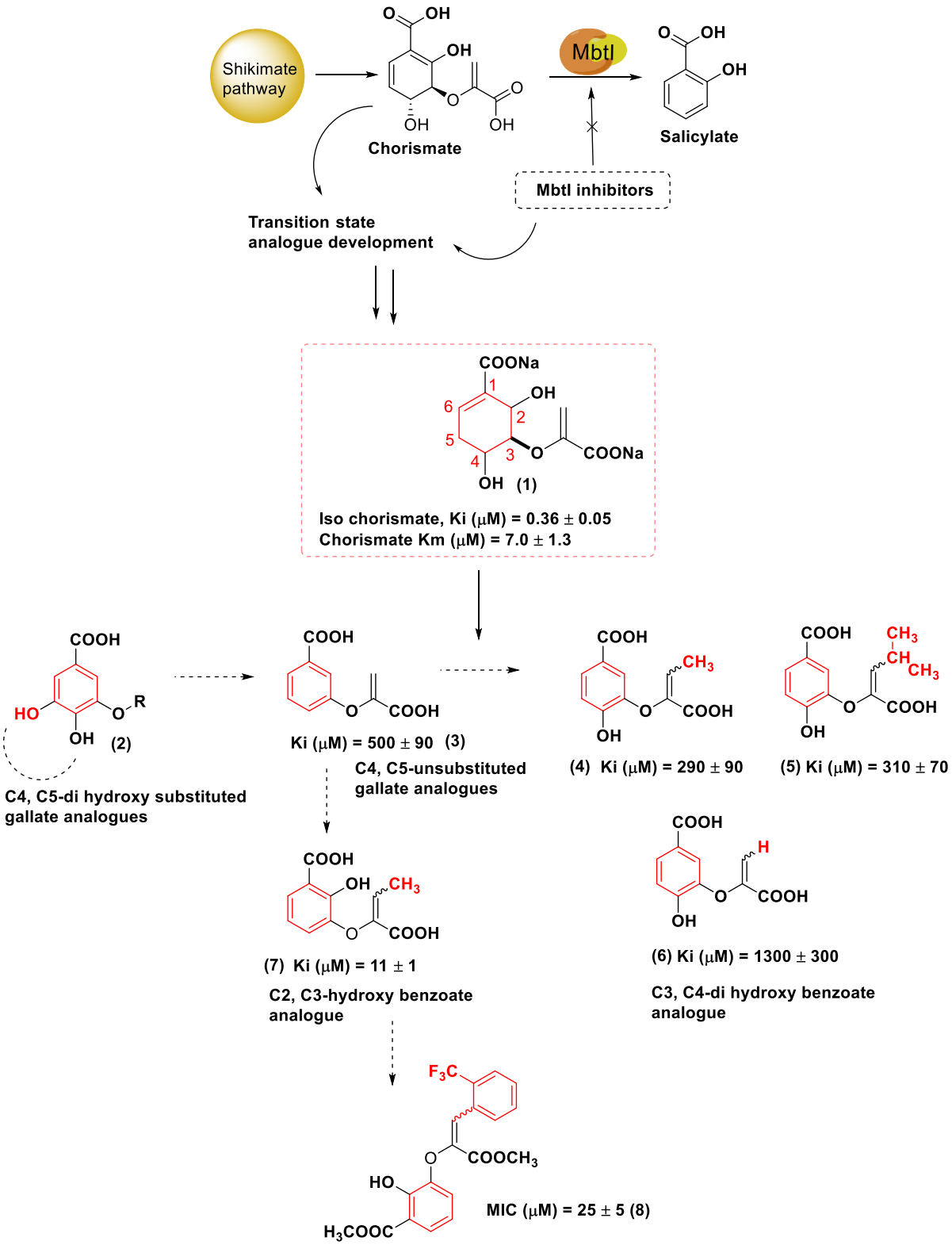

Figure 6. The MbtI enzyme catalyzes the conversion of chorismate to salicylate. TS analogs (**1**-**8**) were developed based on chorismate structure to inhibit mycobactin biosynthesis in its early phases. The figure above depicts the journey from hit compound **1** to the optimized analog **7**, indicating structural modification with a significant MbtI inhibition profile. Other structural modifications (**4**, **5**, and **6**) led to negligible enzyme inhibition activity.

I.a. TS Analogs:

In 1991, Kozlowski and Bartlett[114] first designed and discovered chorismate TS analog (**1**) as a promising isochorismate synthase inhibitor, which produced a K_i value of 0.36 ± 0.05 μM in iso-chorismate inhibition study. This discovery has further stimulated a search for more potent analogs with the same mechanism of action. Manos-Turvey et al.[115] in 2010 synthesized several novel TS analogs based on the gallate scaffold. Modification of the gallate framework, including a dihydroxy substitution on the aromatic ring at the C-4 and C-5 positions (**2**), resulted in derivatives with inferior biological activity. In contrast, the analog devoid of C-4 and C-5 hydroxyl groups at the aromatic ring (**3**) exhibited better enzyme inhibitory activity and antibacterial properties. Subsequently, studies shifted toward the exploration of 3, 4-dihydroxybenzoic acid-based inhibitors. Substitution with small aliphatic groups, such as methyl and isopropyl units, at the C-3 position of the carboxyvinyl residue, yielded better analogs (**4**, **5**) compared to C3-enol-pyruvyl substituted derivative (**6**) in terms of MbtI enzyme inhibitory activity. A moderate improvement in the enzyme inhibition profile was observed in the case of enol-pyruvate linkage substitution at the C-2 and C-3 position of the aromatic ring. Among all the designed analogs, the compound with a 2,3-dihydroxybenzoate scaffold bearing the But-2-enoate (**7**) substitution at the C-3 position showed the most promising inhibitory activity with a K_i value of 11 ± 1 μM against MbtI. However, compound **7** exhibited poor antitubercular activity in whole-cell screens against Mtb, giving an MIC_{50} value >1mM

reported in the study performed by the same research group.[116] Further to this, the same research group designed and evaluated a series of 3-phenylacrylate analogs as MbtI inhibitors. None of the compounds synthesized in this attempt showed improved inhibition profile against MbtI compared to **7,** although analog (**8**) has emerged with a significant *in vitro* antitubercular activity with an MIC_{50} value of 25 ± 5 μM in iron supplemented media.[116] (**Figure 6**)

In 2015 Liu et al.[117] designed TS analog (**9**) based on the parent scaffold **1**. However, this compound exhibited suboptimal MbtI inhibition activity (*i.e.*, <10%) at a concentration of 100 μM. The introduction of a CH_2 moiety as a bioisosteric replacement for the C5 oxygen atom of chorismate resulted in the loss of a critical hydrogen bond with the Arg405 residue in the active site of MbtI enzyme, yielding an inactive analog. Also, introducing a protonated amino group at the C-4 position of the aromatic ring of **9** resulted in a significant repulsive electrostatic interaction with the Arg405 residue, which made an additional negative impact on the enzyme MbtI inhibition activity (**Figure 7**).

In 2017, Zhang et al.[118] designed TS analog (**10**), within which the C2-OH of the parent scaffold **1** was replaced with an amino group. However, analog **10** also failed to exhibit any significant enzyme inhibitory activity, K_i <10% at 100 μM concentration (**Figure 7**).

In 2018, Pini et al.[119] replaced the phenyl ring of compound **7** with a chromane framework and designed a library of novel MbtI inhibitors bearing the benzodihydropyran scaffold. Analog (**11**) exhibited an IC_{50} value of 55.8 ± 4.2 μM in the MbtI enzyme inhibition assay and emerged as the most potent one among the other library members (**Figure 8**).

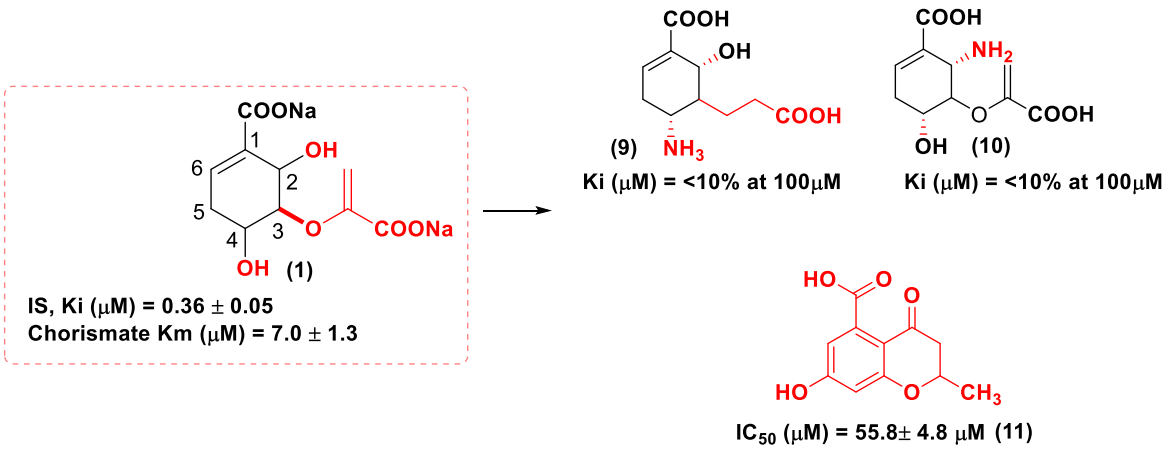

Figure 7. Chemical structure of MbtI inhibitors (**9-11**). The analogs **9** and **10** are based on hit scaffold **1,** whereas the analog **11** is based upon ligand **7**.

I.b. Non-TS Analogs:

In 2010, Vasan et al.[120] designed novel benzisothiazolones, diaryl sulfones, and benzimidazole-2-thione class of compounds as non-TS analogs. The ligand benzimidazole-2-thione (**12**) emerged as the most promising MbtI inhibitor with a K_i value of 5.89 ± 0.27 μM in high throughput enzyme inhibition assays. In 2018, Chiarelli et al.[121] synthesized a series of furan ring-containing MbtI inhibitors based on hits identified through *in-silico* screening of a commercially available library against the crystal structure of MbtI (PDB ID: 3VEH).[122] Hit compound 2-phenyl furan derivative (**13**) was tested *in vitro* in MbtI inhibition assay and showed a K_i value of 21.1 ± 4.1 μM against enzyme MbtI. Therefore, compound **13** was considered as the starting point for further development. SAR investigations into the structure of **13** led to the synthesis of analog (**14**), which carried only one structural difference, *i.e.,* removal of the *o*-chloro group at the aromatic ring and showed MbtI inhibition activity with K_i (μM) of 5.3, albeit with low antitubercular activity (MIC_{99} = 156 μM) against Mbt H37Rv in a whole-cell assay (**Figure 8**). Further, the same research group in 2019,[123] reported a small library of 16 furanic acid analogs with MbtI inhibitory activity. Analog (**15**) with *ortho*, *para*-

di CF_3 substitution on the aromatic ring was the most potent candidate with a K_i value of 3.9 ± 1.7 µM against MbtI inhibition assay and IC_{50} of 13.1 ± 2.0 µM in a whole-cell assay against Mtb H37Rv. Another significant outcome of this study was the discovery of two other derivatives (**16** and **17**), with an *ortho*-CN group substitution on aromatic ring. The only structural difference between the two compounds was a *para* substitution on the aromatic ring. The candidate with additional *p*-CF_3 substitution (**16**) emerged as slightly better analog (K_i = 5.7 ± 1.5 µM, IC_{50} 18.5 ± 3.2 µM) compared to the candidate with *p*-NO_2 substitution (**17**) (K_i = 5.0 ± 1.9 µM, IC_{50} 24.4 ± 5.9 µM). The same group in 2020[124] reported a pilot library of furan analogs with different substitutions at meta-position on the aromatic ring. The study revealed that analog (**18**) with a *m*-CN-group substituted aromatic group showed most promising activity with a K_i value of 3.1 ± 1.0 µM in the MbtI inhibition assay and IC_{50} of 6.3 ± 0.9 µM in a whole-cell assay against Mtb H37Rv. Analog **18** emerged as the most potent competitive inhibitor of MbtI known to date.

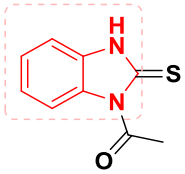

(12) K_i = 5.89 ± 0.27µM

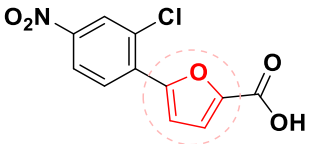

(13) K_i = 21.3 ± 4.3 µM

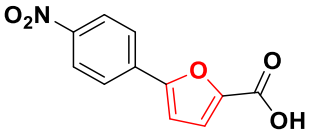

(14) K_i = 18.2 ± 5.1 µM

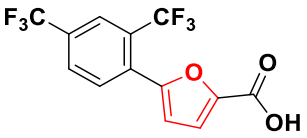

(15) K_i = 3.9 ± 1.7 µM

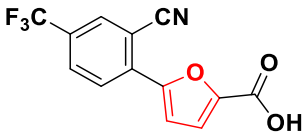

(16) K_i = 5.7 ± 1.5 µM

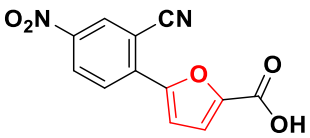

(17) K_i = 5.0 ± 1.9 µM

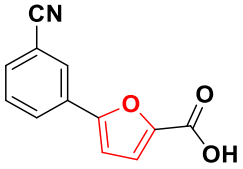

(18) K_i = 3.1 ± 1.0 µM

Figure 8. MbtI inhibitors development comprising the benzimidazole **12** and furan scaffolds (**13**-**18**) with a significant enzyme MbtI inhibition profile.

IIa. Salicyl-AMP ligase (*MbtA*) inhibitors:

MbtA-targeted antitubercular agents so far constitute the dominant class of mycobactin biosynthesis inhibitors. These types of molecules have been designed to target the initial step of the mycobacterial siderophore production catalyzed by MbtA, *i.e.,* activation of salicylate with the formation of salicyl-adenosine monophosphate (Salicyl-AMP) intermediate (**19**). MbtA assembles the mycobactin peptide core and acts as a bifunctional enzyme that converts salicylate into Salicyl-AMP and loads the latter intermediate on to the phosphopantetheinylation domain of MbtB.[107] The majority of MbtA inhibitors are nucleobase-modified adenosine analogs that mimic the Salicyl-AMP structure and block the enzyme activity. However, several non-nucleoside MbtA inhibitors[125] are currently being developed. The archetypal MbtA inhibitor scaffold comprises an aromatic ring, a linker bridge, a sugar unit, and a base moiety. All these structural modifications have been summarized with respect to newer inhibitors' development in the sections below.

***A. Linker modification*:**

Ferreras et al. (2005)[126] reported the design and synthesis of 5′-*O*-*N*-salicylsulfamoyl adenosine (Salicyl-AMS) (**20**), a congener of Salicyl-AMP **19**, as a MbtA inhibitor (**Figure 9**). The molecular framework of ligand **20** resembled that of the naturally occurring intermediate Salicyl-AMP **19**, and the only structural difference was constituted by the sulfonamide linkage

replacing the orthophosphate ester group. Salicyl-AMS, **20** exhibited significant MbtA inhibitory activity with a K_i value of 10.7 ± 2.0 nM and emerged as the first biochemically confirmed inhibitor of siderophore biosynthesis. Salicyl-AMS showed eighteen-fold higher antitubercular activity (MIC_{50} value of 2.2 ± 0.3 μM) against Mtb H37Rv strains, cultured in iron-deprived conditions, compared to bacteria grown in iron-rich media (MIC_{50} value of 39.9 ± 7.6 μM). In 2013,[127] Lun et al. studied ligand **20** in a TB infected acute murine model over four weeks (intraperitoneal administration, 5.6 or 16.7 mg/kg dose) and reported that Salicyl-AMS also did not exhibit any *in vitro* cytotoxicity against P388, HepG2, and Vero cell lines (CC_{50}>200μM). In contrast, the pharmacokinetic (PK) profile of **20** showed that this ligand had poor oral bioavailability (F<2%), low clearance (Cl = 4.9 mL min^{-1} kg^{-1}), low microsomal stability ($t_{1/2}$ >30min), and a small volume of distribution (V_d = 0.079 L. kg^{-1}). Due to suboptimal PK profile, **20** was not taken forward in clinical trials, but the initial *in vitro* and *in vivo* investigations on its efficacy and toxicity profile inspired subsequent drug discovery campaigns by other research groups aiming to develop novel Salicyl-AMS analogs with more favorable metabolic properties and improved PK profile.

Somu et al. in 2006[128] reported the synthesis of Salicyl-AMS analogs with several bioisosteric replacements of the cleavable acyl phosphate linker of **19** and modifications of the salicyl moiety. The compounds were evaluated for their ability to inhibit the growth of Mtb H37Rv under iron-deprived conditions and disrupting the activity of the adenylating enzyme MbtA. These rationally designed MbtA inhibitor nucleosides contained three types of acyl phosphate moiety-mimicking linkages, including acyl sulfamate and acylsulfamide *β*-ketophosphonate, and acyltriazole linkers. Nucleosides containing the *β*-ketophosphonate and acyltriazole tether structural modification failed to exhibit any efficacy against H37Rv at 100 μM concentration. However, the acylsulfamide linker-bearing analog (**21**), obtained by substituting the oxygen atom of the sulfamate group with a nitrogen atom, showed notable activity in whole-cell assays,

with an MIC_{99} value of 0.19 μM, similar to that of isoniazid (MIC_{99}= 0.18 μM), and an MIC_{50} value of 0.077 ± 0.022 μM under iron-deficient medium.

Analog **21** was assessed for mycobactin biosynthesis inhibitory activity using a modified radioassay method, adapted from the one reported by DeVoss et al.[107] In this comparative study, complete inhibition of mycobactin and carboxymycobactin biosynthesis was observed at a concentration of 10 μM. In 2006,[129] Vannada et al. further evaluated the MbtA inhibition activity of nucleoside **21** using a [^{32}P] PPi-ATP exchange assay and showed that the ligand **21** was a potent MbtA inhibitor with K_i value of 0.0038 ± 0.0006 μM (**Figure 9**). Furthermore, hydrolysis of the acylsulfamide linkage of derivatives **20** and **21** led to the production of cytotoxic metabolites (**22** and **23**)**,** and ionization of the sulfamate linker at physiological pH resulted in limited oral bioavailability (**Figure 9**).

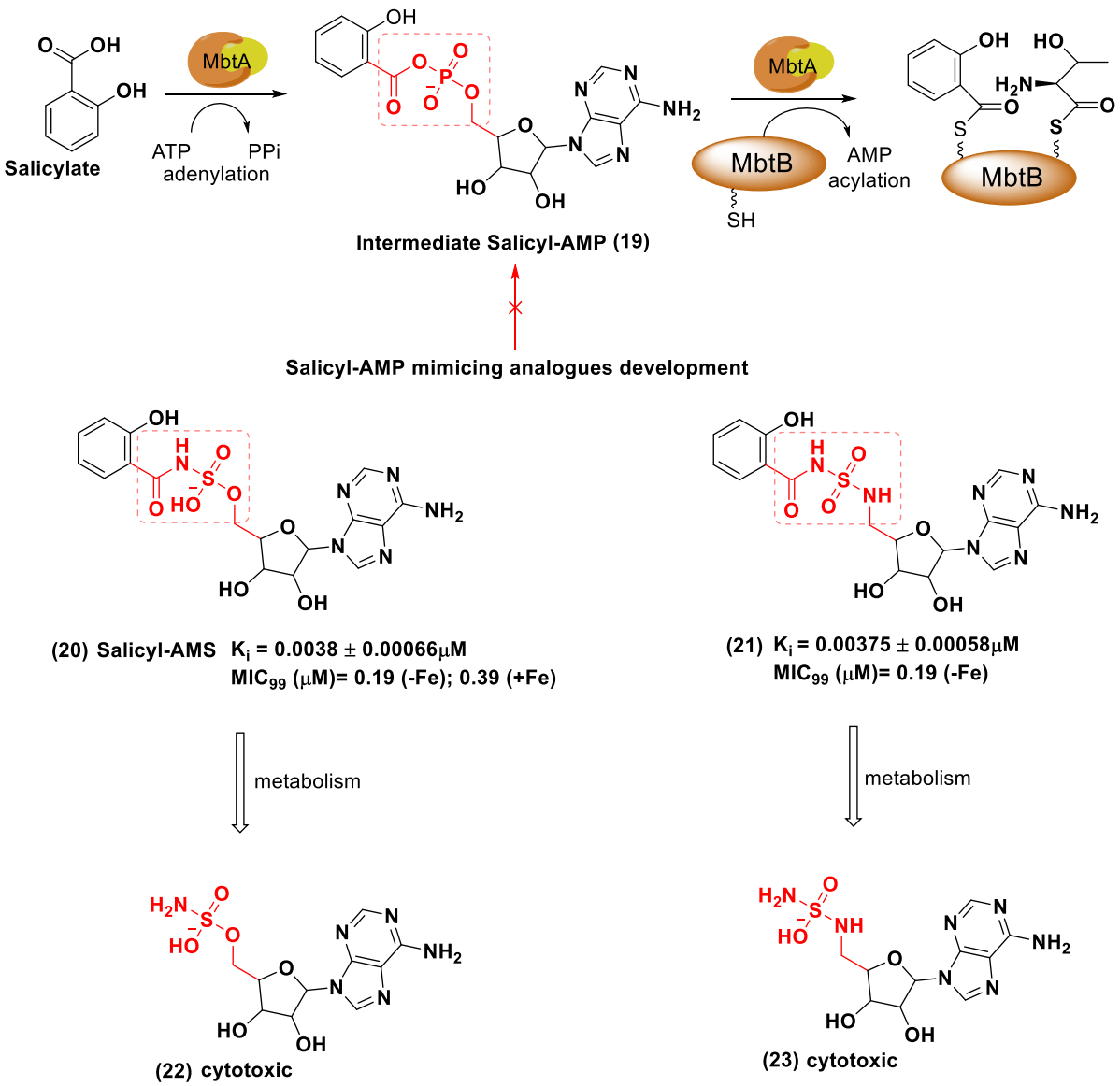

Figure 9. MbtA is a bifunctional enzyme that catalyzes the conversion of salicylate to Sal-AMP (**19**) and the loading of **19** onto the MbtB thiolation domain. The first MbtA inhibitor developed to target the Salicyl-AMP biosynthetic step was Salicyl-AMS **20**. This lead compound **20** exhibited a remarkable antitubercular activity in iron-efficient (+Fe) and iron-deprived (-Fe) medium, although its PK profile was suboptimal. This prompted further studies to discover analogs with more favorable PK parameters and drug-like properties, such as nucleoside **21**, without compromising their Mtb H37Rv-growth inhibitory activity. Hydrolysis

of the acylsulfamide linkage of derivatives **20** and **21** resulted in cytotoxic metabolites **22** and **23**.

Vannada *et al.*[129] further modified the linker unit of the antitubercular nucleosides by substituting the labile acylsulfamate moiety of **21** with the more chemically stable *β*-ketosulfonamide linker (**Figure 10**). However, this structural modification yielded nucleoside (**24**) and fluorinated analog (**25**) with poor drug-like properties with K_i values of 3.30 ± 0.57 and >100μM against MbtA, respectively, compared to the parent acylsulfamide derivative **21**. This approach has not been taken further into consideration for analog development.[129]

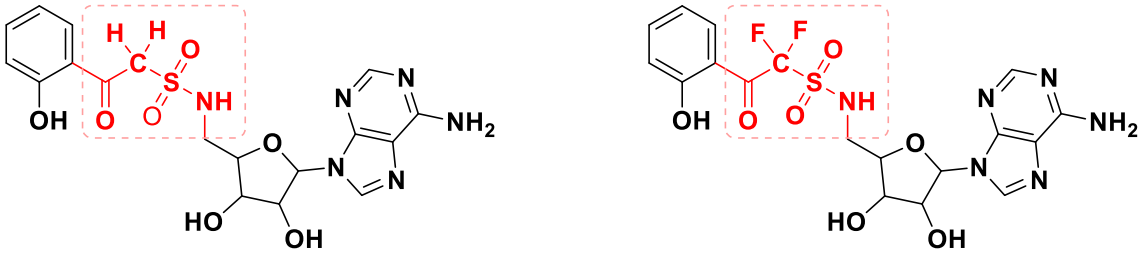

(24) K_i (μM) = 3.30 ± 0.57
MIC_{99} (μM) = 25

(25) K_i (μM) = >100
MIC_{99} (μM) = >100

Figure 10. Chemical structures of analogs **24** and **25** with respective MbtA inhibition values and antitubercular profile in iron-deprived GAST medium. The major structural modification carried out with the *β*-ketosulfonamide linker resulted in poor candidate development.

In 2006,[130] Miethke et al. designed and synthesized several aryl sulfamoyl adenosine analogs of Salicyl-AMS and tested their inhibitory activity against 2,3-dihydroxybenzoate-AMP ligase (enterobactin synthetase component E or DhbE). This enzyme is involved in the synthesis of DHB-capped siderophores, termed bacillibactins, produced by *Vibrio* spp, *Bacillus* spp, and

other enteric bacteria. Sal-AMS **20** exhibits inhibitory activity against this enzyme. The compounds were tested at a concentration of 12.5 μM, and the nucleosides containing hydroxamoyl linkage (BEN-AMN, **26**) showed only 1.8% of DhbE inhibition compared to Sal-AMS, which showed 99.6% inhibition. This weak activity was attributed to the shortening of the hydroxamoyl linker leading to impairment of the fitting of the aryl or adenosine moiety to the DhbE active site. Notably, a derivative bearing the dihydroxybenzoyl-sulfamoyl linkage (DHB-AMS) inhibited the enzyme marginally better than Sal-AMS **16**, with 99.8% inhibition. Further introduction of a fluorine atom in the aromatic ring resulted in an inactive analog F-BEN-AMN (**27**) that showed only 0.1% of DhbE inhibition at 12.5 μM concentration. Further research in this direction was ceased (**Figure 11**).

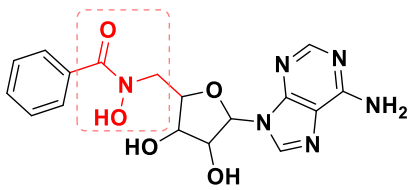

(26) DhbE inhibition 1.8% at 12.5μM concentration

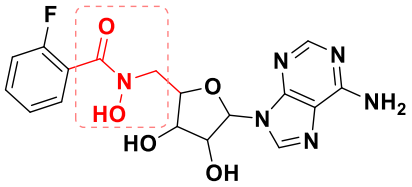

(27) DhbE inhibition 0.1% at 12.5μM concentration

Figure 11. Chemical structures and enzyme DhbE inhibition profile of BEN-AMN **26** and F-BEN-AMN **27**.

In 2007,[131] Qiao et al. first suggested the introduction of the urea linker to connect the adenosine unit with the *o*-hydroxy phenyl ring. This resulted in acyclic acyl urea derivative (**28**) and in a nucleoside (**29**), in which a chromane scaffold was linked via an amide bond to the sulfamoyl unit of Salicyl-AMS (**Figure 12**). Analog **28** showed a 329-fold loss of antitubercular potency (K_i = 1.25 ± 0.05 μM) compared to Salicyl-AMS **20**. Analog **29** also exhibited poor activity with a K_i value of >100 μM against MbtA.

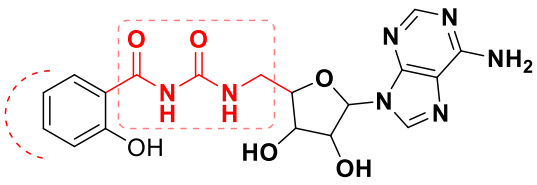

(28) K_i (μM)= 1.25 ± 0.05
MIC_{99} (μM)= 200 (-Fe); >200 (+Fe)

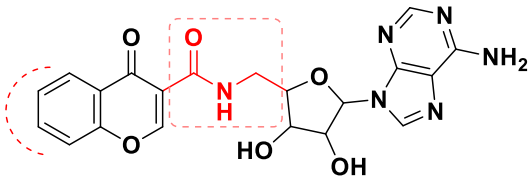

(29) K_i (μM)= >100
MIC_{99} (μM)= 12.5-25 (-Fe); 50 (+Fe)

Figure 12. Chemical structures and antitubercular profile of analogs **28** and **29** with diamide and amide linkage, respectively.

In 2013,[132] Engelhart and Aldrich designed four conformationally constrained analogs of Salicyl-AMS **20** with linker modification by introducing chromone, quinolone, benzoxazinone-3-sulfonamide, and 8-hydroxy chromane units into the framework of parent compound **20** to remove two rotatable bonds and the ionizable sulfamate group. This synthetic strategy is aligned with the observations by Veber et al.,[133] who suggested that reduced molecular flexibility of drug candidates can be an important predictor of good oral bioavailability the sulfonamide linkage of adenosine with the chromane (**Figure 13**) scaffold yielded nucleoside (**30**), that showed non-promising activity against Mtb H37Rv in both iron-deficient conditions (MIC_{99} = >50 μM) and iron-rich media (MIC_{99} = >50 μM). The lack of an ionizable functional group in the nucleoside derivative **30** led to a significant reduction in inhibitory activity against the MbtA enzyme with K_i value of 0.12 ± 0.02 μM. This linker modification was not taken into account further as part of favorable design efforts in subsequent studies.

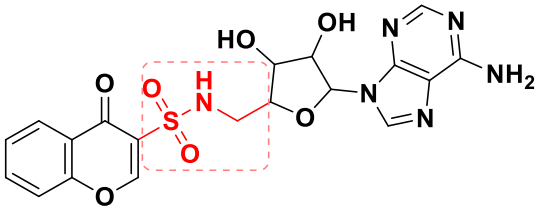

(30) Ki^{app} (μM)= 0.12 ± 0.02
MIC_{99} (μM)= >50 (-Fe); >50 (+Fe)

Figure 13. Chemical structure and antitubercular profile of conformationally constrained nucleoside analog **30**. Two major structural modifications have been considered **(a).** constrained sulfonamide linkage introduction, and **(b).** replacement of the aromatic ring with chromane moiety. All these modifications resulted in poor candidate development.

B. Aromatic group modification:

The *ortho*-hydroxyl group within the salicylate residue is another important structural feature necessary for the biological and biochemical activity of Salicyl-AMS analogs. The different design approaches indicate that removal or substitution of the hydroxyl group with another group considerably affects the enzymatic inhibitory activity and antitubercular properties when compared to parent ligand Sal-AMS **20**. Besides the *ortho* position, substitution at other positions, *i.e., meta* or *para* or di-substitution approaches, should also be accounted for in newer candidate development purposes. In their early work, Somu et al.[128] observed that Salicyl-AMS analogs containing a 2-amino benzoate residue (**31**) or an unsubstituted benzene ring (**32**) showed complete ablation (MIC_{99} >100 μM) or significant reduction, respectively, (MIC_{99} = 12.5 μM) of Mtb H37Rv growth inhibitory properties (**Figure 14**).

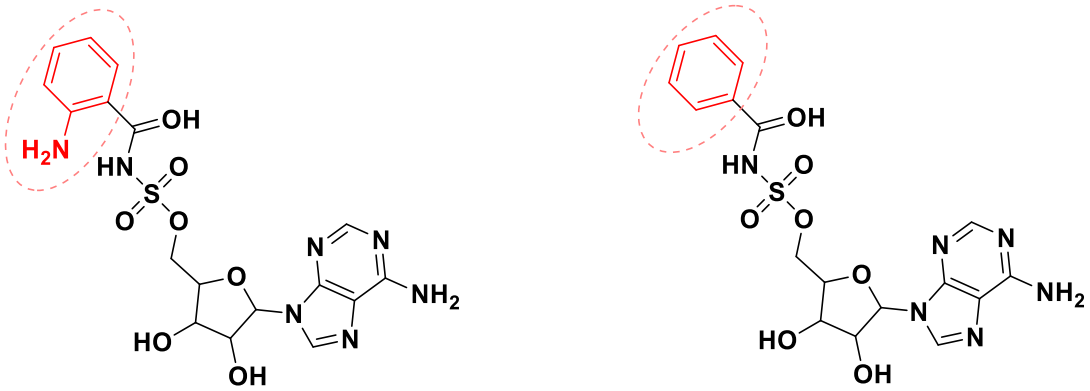

Figure 14. Chemical structures and antitubercular profile of analogs **31** and **32**

Following these studies, Qiao et al. in 2007[131] further explored the importance of substitution at the C-2 position of the salicyl moiety. These authors found that the C2-hydroxy group was essential for antitubercular efficacy. Fluoro-substitution at the C4 position of the aromatic ring yielded compounds (**33**), with significant growth inhibitory activity in whole-cell screening against Mtb H37Rv under iron-limiting conditions (MIC_{99} = 0.098 μM) compared to iron-rich conditions (MIC_{99} = 0.39 μM). Analog **33** exhibited a significant MbtA inhibition activity with a K_i value of 0.012 ± 0.0016 μM. Derivative (**34**) bearing an additional C4-amino group on the aromatic ring showed improved enzyme inhibition activity (K_i = 0.040 ± 0.004 μM) and promising selectivity against Mtb grown in the iron-deprived medium compared to Mtb cultured in an iron-rich environment, with MIC_{99} values of 1.56 μM and 25 μM, respectively. Nelson et al.[134] performed PK profile studies on **34**. The poor AUC_{po} and C_{max} data gathered for this compound indicated that the presence of the *para*-amino group enhanced polarity and led to a faster clearance (**Figure 15**).

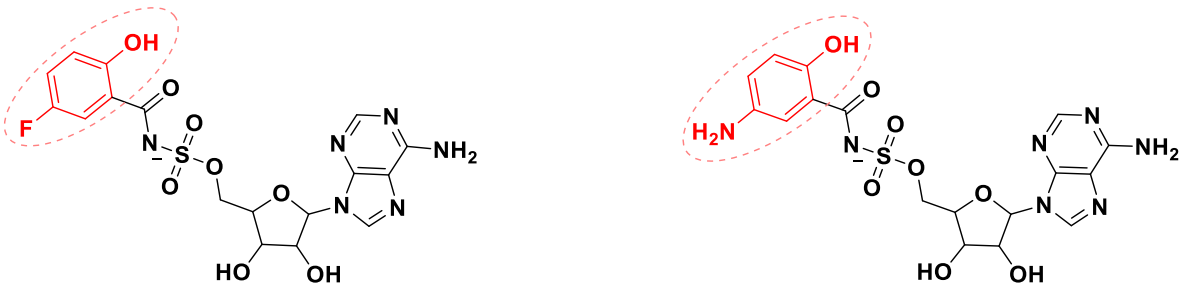

Figure 15. Chemical structures and antitubercular profile of analogs **33** and **34**. Di-substituted aromatic scaffold-comprising analogs emerged as promising candidates.

In contrast, substitutions of the salicyl moiety with morpholine (**35**), cycloalkyl (**36** and **37**), alkyl (**38**), alkyloxy (**39**), methoxymethane (**40**)**,** and aminoacyl (**41**) units were poorly tolerated yielding nucleoside derivatives weakly active against the tubercle bacillus H37Rv (**Figure 16**).[131] The Qiao research group also designed and developed some pyridyl analogs (**42** and **43**) with different substitutions at the second position of the heterocyclic ring, yielding a derivative containing a tetrafluoro 4-azido benzene moiety (**44**). However, this synthetic approach failed to elicit the desired inhibitory effects both in whole-cell screening (MIC_{99}> 200 μM against Mtb in iron-deficient and replenished conditions) and enzymatic assay levels. As an exception, the pyridine analog (**45**) with chlorine substitution at the second position of the heterocyclic ring showed moderate antitubercular and MbtA inhibition activity. Compound **45** can be further considered as the lead for the development of better candidates (**Figure 16**).

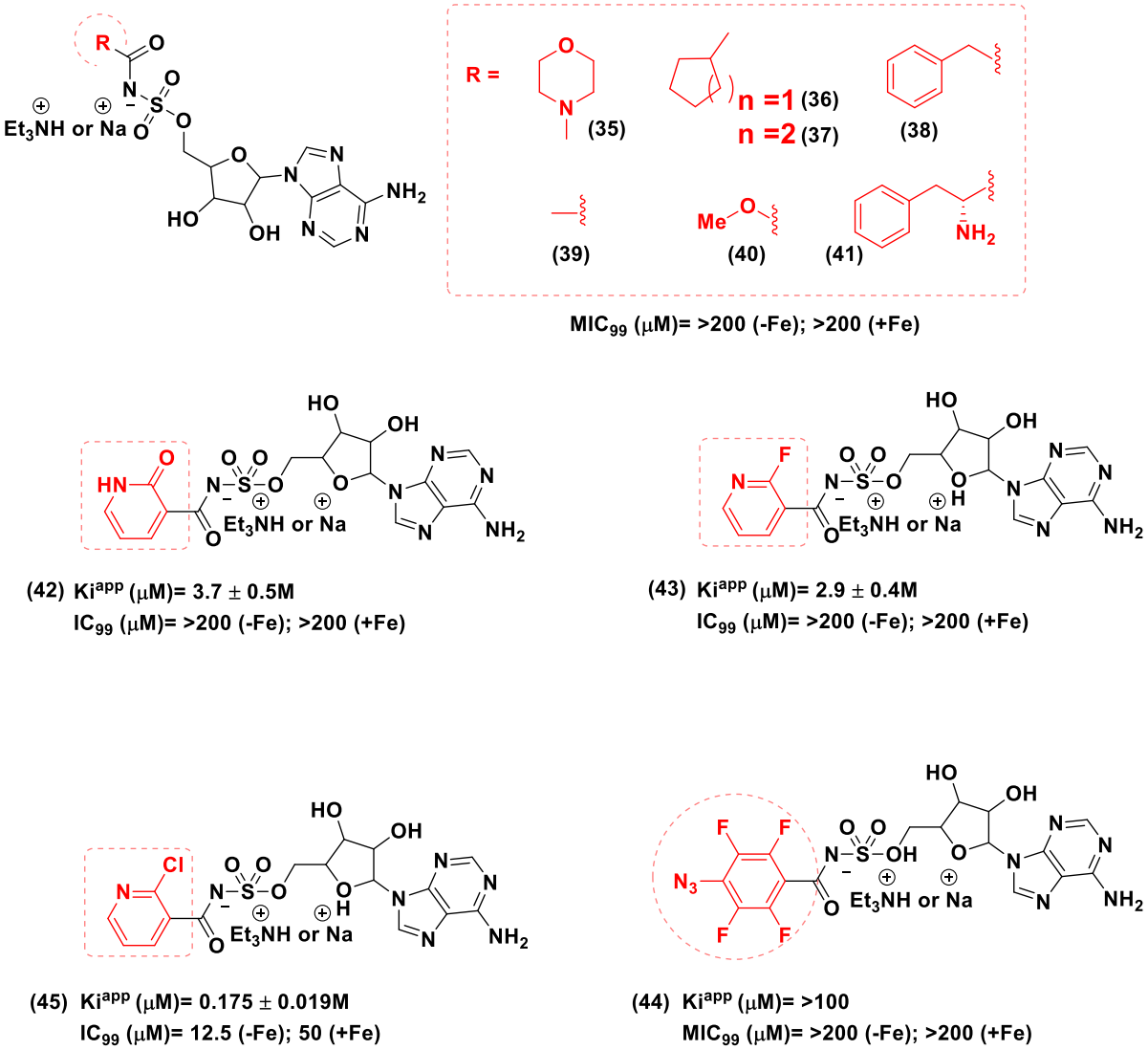

Figure 16. Chemical structure and antitubercular profile of analogs **35-45.**

Engelhart et al.[132] developed conformationally constrained Salicyl-AMS analogs. Design strategy involved incorporating constrained linkers tethering bulkier heterocyclic rings, such as chromone, quinolone, and benzoxazinone-3-sulfonamide units, as the replacement of the *o*-hydroxy aromatic ring. Parent chromane analog **30** has already been discussed in the Sal-AMS linker modification section of this review. The constrained linker-nucleosides series designed by Engelhart et al. included analogs bearing 8-hydroxy chromone (**46**), benzoxazinone-3-sulfonamide (**47**), and quinolone (**48**) moieties. Quinolone-including nucleoside **48** showed a

MbtA enzyme inhibitory activity with a K_i value of 120 nM. This activity can be attributed to the ionizable nitrogen proton of the heterocyclic ring (pK_a = 7.8 circa). However, this compound **48** was not active against Mtb in whole-cell screens. At this stage, it became apparent that the formal negative charge carried by the sulfamate nitrogen of Sal-AMS, **20** was necessary for binding the MbtA active pockets and that a pK_a value closer to that of the parent compound (pK_a of **20** = 3 circa) was key to successful membrane permeability (**Figure 17**).

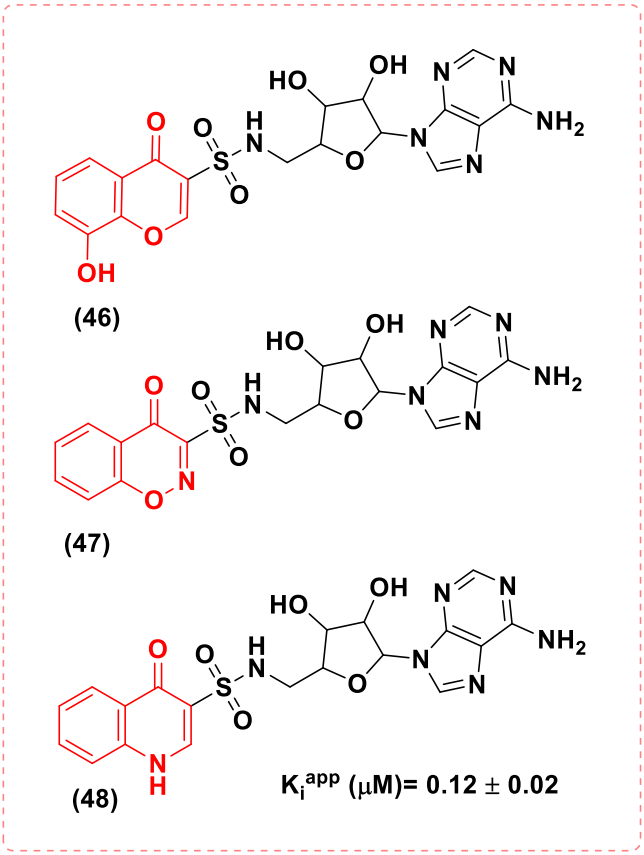

Figure 17. Chronological development order of bulky aromatic substituted nucleosides comprising chromane **46**, benzoxazinone-3-sulfonamide **47**, and quinolone **48** group, respectively. Analogs **46**, **47**, and **48** were synthesized to address the poor PK profile of the

parent compound **20**. Among the series, quinolone analog **48** showed a significant enzyme MbtA inhibition profile.

These challenges encountered in the development of optimal nucleoside MbtA inhibitors were addressed by Dawadi et al.[135] who designed other conformationally constrained Salicyl-AMS analogs using the cinnolone scaffold (**49**). Cinnolone-bearing analogs showed superior antitubercular profile and drug-like properties compared to benzoxazine **47** and quinolone **48**-containing compounds. The halogenated 7-fluorocinnolone analog (**50**), which had a pK_a of 6.3, showed the most promising antitubercular activity (MIC = 2.3 μM) under iron-deficient conditions among the designed derivatives and inhibited MbtA with a K_i of 12 nM (**Figure 18**). PK profile analysis of **50** indicated a seven-fold higher volume of distribution in the female Sprague-Dawley rat model, resulting in a two-fold improvement of half-life compared to Salicyl-AMS **20**. The results were encouraging and favored the use of cinnolone moiety as a bioisosteric replacement of salicyl-sulfamate to provide MbtA inhibitor nucleosides with an improved PK profile.

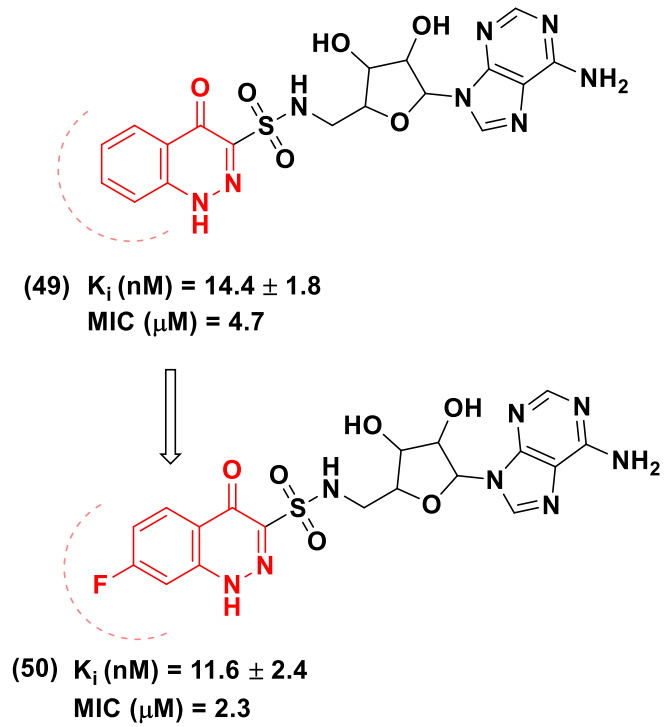

Figure 18. The chromone, quinolone, and cinnolone scaffolds provided a suitable alternative to the ortho-hydroxy benzoate unit and corresponding Salicyl-AMS **20**. The fluorinate cinnolone-containing ligand **50** was found to retain the essential antitubercular activity and MbtA inhibitory property of **20** with an improved PK profile.

C. Sugar moiety modification:

The structural modification of the sugar moiety, combined with alterations at the linker and aromatic nucleus sites, played a crucial role in developing Salicyl-AMS **20** analogs with enhanced MbtA inhibition potency and antitubercular properties.

Early SAR[136] explorations of the glycosyl moiety of Salicyl-AMS **20** revealed that deletion of hydroxyl groups in the ribose sugar and replacement of the sugar moiety with a pentane ring was well tolerated. Derivatives containing a carbocyclic unit (**51**) and 3′-deoxyribose unit (**52**) exhibited excellent antitubercular activity in the whole-cell assay against Mtb H37Rv in iron-

deprived conditions. Both compounds had a MIC_{99} value of 1.56 μM, which represented a 5-fold decrease in activity compared to **20**. These two nucleoside derivatives (**51** and **52**) also displayed potent MbtA inhibition with a 2–3 fold increase in activity compared to Sal-AMS, with K_i values of 2.3 and 3.3 nM, respectively (**Figure 19**).

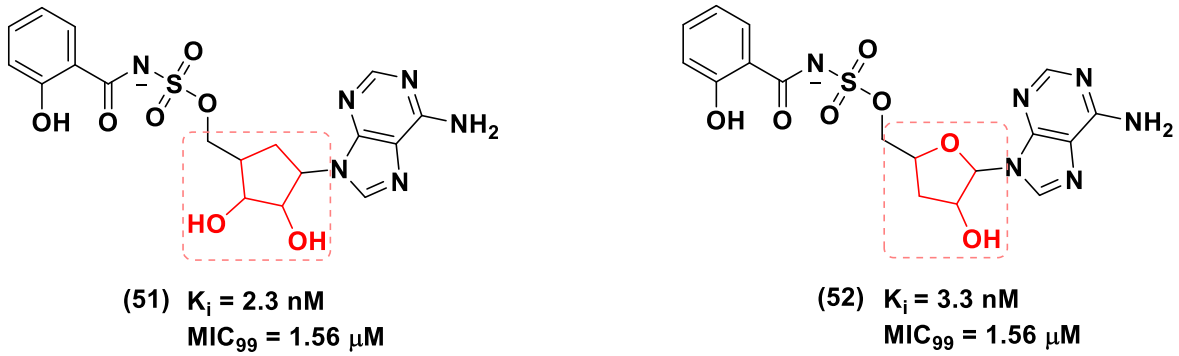

Figure 19. Chemical structure and antitubercular profile of analogs **51** and **52**.

Nelson et al. (2015)[134] reported ligands, which contained a fluorinated ribose sugar unit and the acylsulfamide linker of **21**, including derivatives (**53**) and (**54**) with improved PK profiles and MbtA enzyme inhibitory activity. To address the potential shortcomings of **21**, Nelson and co-workers synthesized several analogs of this compound to improve its poor drug-like properties by modifying their physicochemical properties, such as acidity and lipophilicity. The authors also performed a complete *in vivo* PK evaluation of the compounds in the Sprague-Dawley rat model. The replacement of the 2′- hydroxyl group with fluorine gave compound **53** and additional removal of the 3′- hydroxyl group in the ribose unit afforded analog **54**. Compounds **53** and **54** showed a 3-fold improvement in oral exposure with a 3- and 6-fold increase in half-life, respectively, compared to parent ligand Salicyl-AMS. The replacement of the 2'-hydroxyl group with a fluorine atom resulted in a dramatic improvement in the half-life that translated to the improved oral exposure (**Figure 20**).

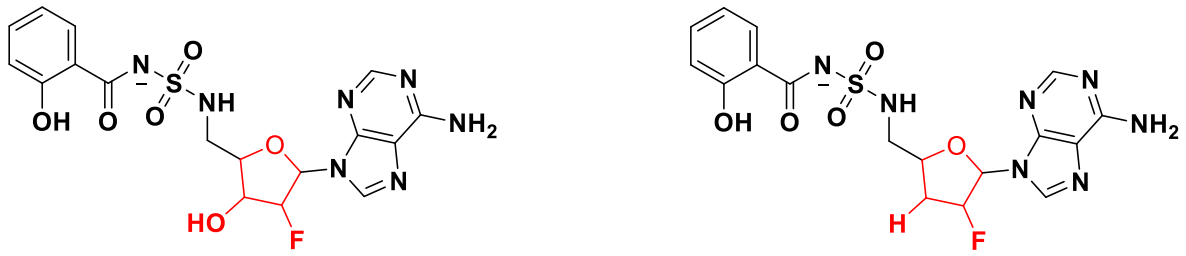

Figure 20. Chemical structures and antitubercular profiles of analogs **53** and **54.** Analogs with fluoro-substituted sugar moiety showed favorable antitubercular and MbtA inhibition properties, and an improved PK profile compared to **21**.

Dawadi et al.[137] further explored the contribution of the fluorinated ribose unit to the antitubercular activity, enzyme inhibition efficacy, and drug disposition profile of the MbtA nucleoside inhibitors, by incorporating fluorine atoms at both 2′ and 3′ positions of the glycosyl unit. Incorporation of fluorine profoundly affected the stereoelectronic properties of the nucleosides' ribose moiety, orienting the sugar ring into either a 2′-*endo*, 3′-*exo* (South), or a 3′-*endo*, 2′-*exo* (North) conformation (**Figure 21**). Compound (**55**), which had the ribose unit in the North (C3′-*endo*) conformation, showed notable activity in the biochemical and whole-cell assays (K_i = 1.4 nM, MIC = 0.78 μM), whereas derivative (**56**) with the South (C2′-*endo*) conformation showed an improved PK profile as evaluated using an *in vivo* cannulated rat model. Derivative **56** showed a four-fold increase in bioavailability (F% 5.3 ± 1.3), fifteen-fold improvement in C_{max}, a 75-fold increase in oral AUC, and a twenty-five-fold greater half-life compared to the lead analog **20**.

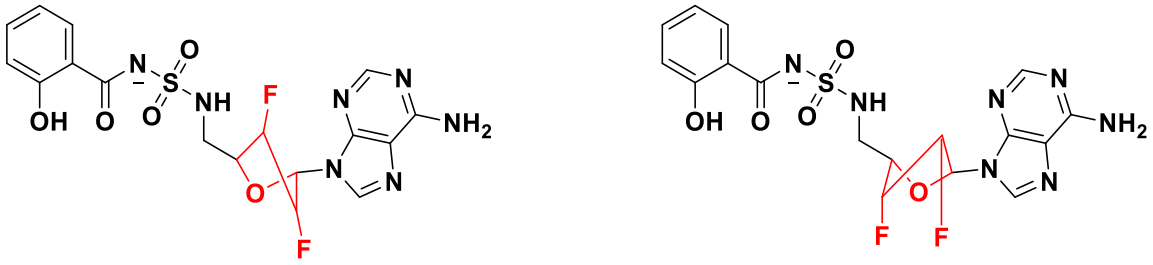

Figure 21. Strategies developed by the Aldrich group toward the modification of the sugar moiety of MbtA nucleosides. Adding two fluorine atoms at positions 2′ and 3′ of the sugar ring resulted in different configurations, e.g., a 3′-*endo*, 2′-*exo* (North, **55**) or a 2′-*endo*, 3′-*exo* (South, **56**), resulted in a significant improvement of pharmacokinetic profile.

In 2016, the Dawadi group[138] sought to improve the bioavailability of promising derivative **53**, and used a prodrug approach to protect the 3′-hydroxyl unit from detrimental pre-systematic hydrolysis by intestinal esterases. Different linear and branched alkanoyl groups, such as methyl (**57**), ethyl (**58**), *n*-propyl (**59**), *n*-butyl (**60**), *n*-heptyl (**61**), *n*-undecyl (**62**), isopropyl (**63**), and 3-pentyl (**64**) ester linkages were incorporated at the 3′-position of the 2′-fluorinated analog **53** to produce a series of lipophilic ester prodrugs (**Figure 22**). Although the prodrugs were stable in mouse, rat, and human serum, the compounds exhibited reduced permeability (apical-to-basolateral direction) in the Caco-2 cell transwell model with 5–28 times higher efflux ratio compared to **53**. This prodrug strategy did not yield the desired results, as it led to a lower oral availability than **53**.

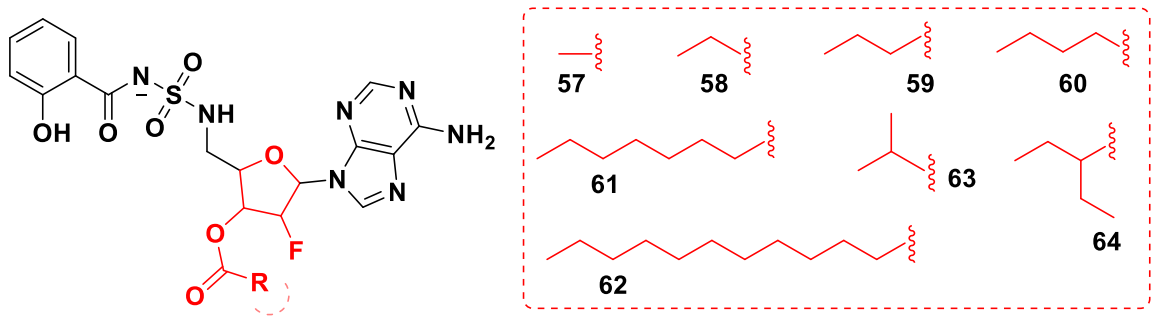

Figure 22. Chemical structure of the ester analogs **57-64** of parent compound **53**.

***D. Base modification*:**

The systematic modifications of the nucleobase unit of Salicyl-AMS **20** and their effects on MbtA inhibition and anti-tuberculosis activity of the resulting derivatives is discussed in this section. In 2008, Neres et al.[139] reported the exploration of SARs of the purine ring. Several analogs of **20**, bearing substitutions at the N1, N3, N7, C2, C6, and C7 positions of the adenine residue were synthesized and evaluated for their biochemical and biological properties. The study revealed that the elimination of N1, N3, or N7 in the adenine unit (**65**) led to decreased MbtA inhibitory potency and antitubercular activity against Mtb H37Rv in iron-deficient conditions. In contrast, removal of the amino group (-NH_2) at the C6 position resulted in inactive analog (**66**), as at least one hydrogen bond donor was crucial for the activity for these types of nucleosides. The insertion of bulky substituents at the purine C6 position, including NH-cyclobutyl and NH-cyclopentyl residues, yielded compounds devoid of any MbtA inhibitory properties and antitubercular activity. Interestingly, compound (**67**), which included the smaller NH-cyclopropyl residue at C6, exhibited a 3.5-fold increase in MbtA inhibitory activity compared to **20** (**Figure 23**). Insertion of bulky aromatic substituents at the C2 position of the purine ring, e.g., 2-phenylamino, phenylethynyl, and 2-phenyl moieties yielded compounds (**68**, **69,** and **70**) respectively, which were up to 24 times more potent than **20**.

Molecular modeling studies corroborated these findings and showed that the active site of the MbtA carries additional space near the adenine-C2 position of the nucleosides, and large aromatic substituents, such as phenyl rings, can be accommodated in the pocket. Compounds **68, 69,** and **70** exhibited significantly improved whole-cell antitubercular activity (MIC_{99} = 49 nM in iron-deficient environment) and MbtA-binding properties (K_i values ranging from 0.27 - 0.94 nM) compared to **20** (**Figure 23**).

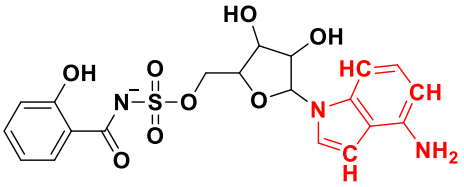

(65) K_i (nM) = 20.1 ± 2.3
MIC_{99} (μM) = 6.25 (-Fe); 50 (+Fe)

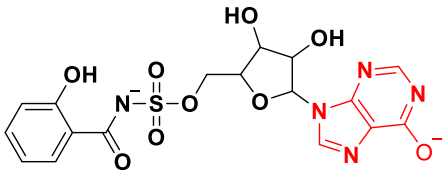

(66) K_i (nM) = 800 ± 50
MIC_{99} (μM) = >100 (-Fe); >100 (+Fe)

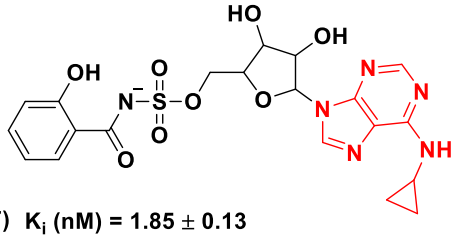

(67) K_i (nM) = 1.85 ± 0.13
MIC_{99} (μM)= 0.098 (-Fe); 6.25 (+Fe)

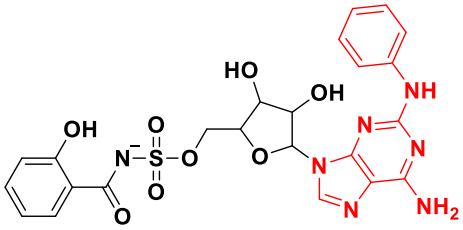

(68) K_i (nM) = 0.94 ± 0.16
MIC_{99} (μM) = 0.049 (-Fe); 0.39 (+Fe)

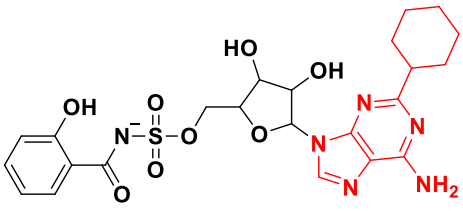

(69) K_i (nM) = 0.40 ± 0.05
MIC_{99} (μM) = 0.049 (-Fe); 0.39 (+Fe)

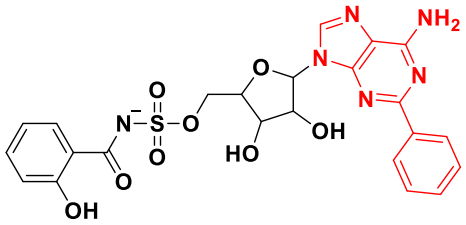

(70) K_i (nM) = 0.27 ± 0.07
MIC_{99} (μM) = 0.049 (-Fe); 0.39 (+Fe)

Figure 23. Base modification of Salicyl-AMS scaffold resulted in some novel biologically efficient analogs (**65-70**).

Nelson et al.[134] conducted further purine ring modifications to improve the PK profile of hit compound **21**. Among the nucleoside analogs reported by the group in 2015, three derivatives carrying base moiety alterations were explicitly designed to improve enzyme inhibition, antimycobacterial activities, and enhance PK profile. Substitutions at C2 and C6-*N* position of the adenyl group yielded N^6-cyclopropyl and N^6-cyclopropyl-2-phenyl derivatives (**71** and **72**), respectively, and the inclusion of an NH-cyclo-propyl moiety at C6 of the purine ring greatly enhanced antitubercular activity compared to the parent compound **21**. However, nucleoside **72**, which carried a further C2-phenyl substitution, showed a 16-fold reduction in antitubercular activity but improved MbtA inhibitory properties (K_i = 0.76 ± 0.40 nM) compared to **21**. Additional structural modifications of the parent scaffold **21**, *i.e.*, the inclusion of a fluorine atom at the C2′ position of the sugar unit and C8-phenyl substitution at the adenine moiety, led to analog (**73**), which exhibited improved MbtA inhibitory property with a K_i value of 1.6 ± 0.1 nM and approximately 8-fold decrease in antitubercular activity. These structural modifications resulted in cLogP values from 0.89 (**21**) to 0.5 and 2.9 for analogs **71** and **72**, respectively (**Figure 24**).

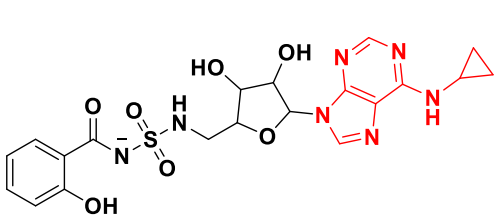

(71) K_i **(nM) = 1.5 ± 0.2**
MIC (μM) = 0.098

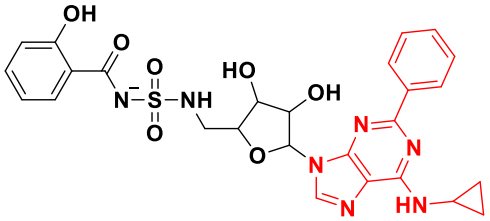

(72) K_i **(nM) = 0.76 ± 0.40**
MIC (μM) = 6.25

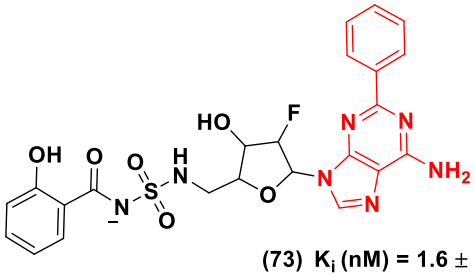

(73) K_i **(nM) = 1.6 ± 0.1**
MIC (μM) = 1.56

Figure 24. Chemical structures and antitubercular profiles of the base-modified nucleoside analogs **71-73**.

Krajczyk et al.[140] further expanded the SARs of base-modified Salicyl-AMS analogs and designed and evaluated a series of derivatives containing the isosteric 8-aza-3-deazaadenine unit that was substituted at its C2 position with various aryl groups. The alteration of the Salicyl-AMS **20** adenosine scaffold led to analogs, such as compounds (**74** and **75**), which were able to achieve MbtA inhibition with K_i values ranging from 6.1 to 25 nM and arrest the growth of Mtb with minimum inhibitory concentrations ranging from 12.5 to >50 μM.

These findings indicated that bioisosteric replacement of the purine ring and C2-aryl substitution led to a significant decrease in the efficacy profile of the derivatives (**Figure 25**).

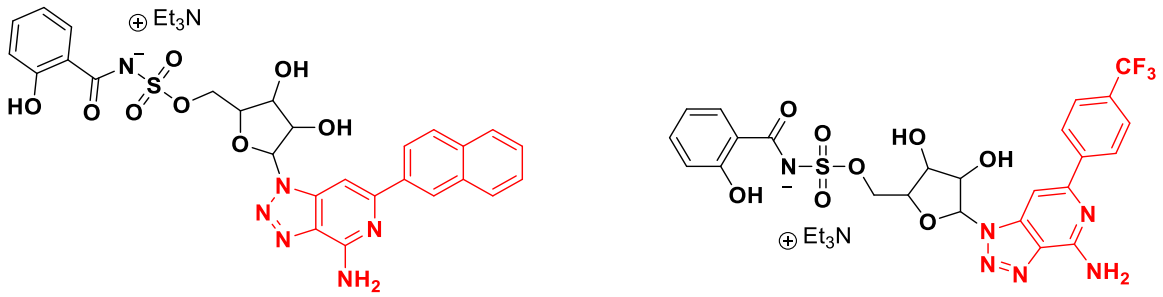

Figure 25. Chemical structures and antitubercular profiles of base-modified nucleoside analogs **74** and **75** incorporating 8-aza-3-deazaadenine as a bioisosteric replacement of the adenine ring.

In a joint research project between Tan and Quadri et al.[108] two novel Salicyl-AMS derivatives, Salicyl-AMSNMe (**76**) and Salicyl-6-MeO-AMSN (**77**), were reported. The groups investigated the SARs of the base- and linker-modified nucleotides (**Figure 26**).

The compounds were tested for antimycobacterial activity against a strain of the non-pathogenic *Msmeg* (ΔEM-pMbtA$_{tb}$) engineered to be susceptible to MbtA inhibitors in a MbtA$_{tb}$-dependent manner. The study revealed that **77**, which was devoid of the purine C6 amino motif of Salicyl-AMS **20**, exhibited an almost 6-fold decrease in antimycobacterial activity compared to **20** (MIC = 0.8 ± 0.2 μg/mL in iron-depleted conditions) with MIC values of 5.3 ± 1.3 μg/mL and >64 μg/mL in GAST and GAST-Fe medium, respectively. Salicyl-AMSNMe showed an antimycobacterial activity comparable to Salicyl-AMS. The study also revealed that the MbtA inhibitory efficacy of Salicyl-6-MeO-AMSN was significantly lower compared to **20** (K_i = 26.6 ± 2.5 nM) with a K_i value of 277.1 ± 12.2 nM, suggesting that the presence of the adenosine C6-NH_2 group in nucleoside-based MbtA inhibitors is crucial for the optimal biological activity for this class of compounds.

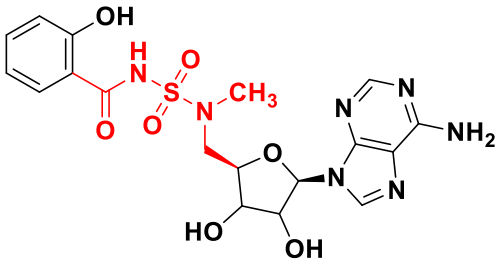

(76) K_i (nM) = 158.5 ± 8.1
MIC (μM) = 0.8 ± 0.2 (-F); >64 (+Fe)

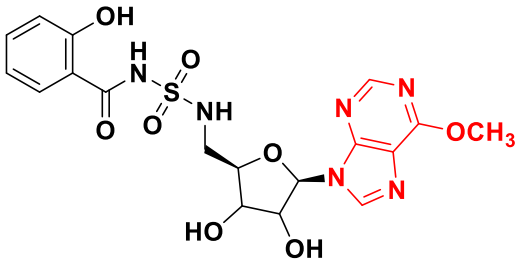

(77) K_i (nM) = 277.1 ± 12.2
MIC (μM) = 5.3 ± 1.3 (-F); >64 (+Fe)

Figure 26. Chemical structure and antitubercular profile of salicyl-AMSNMe **76** and Salicyl-6-MeO-AMSN **77**.

The major and most significant structure-activity relationship (SAR) findings related to Salicyl-AMS MbtA inhibitors are summarized in **Figure 27**.

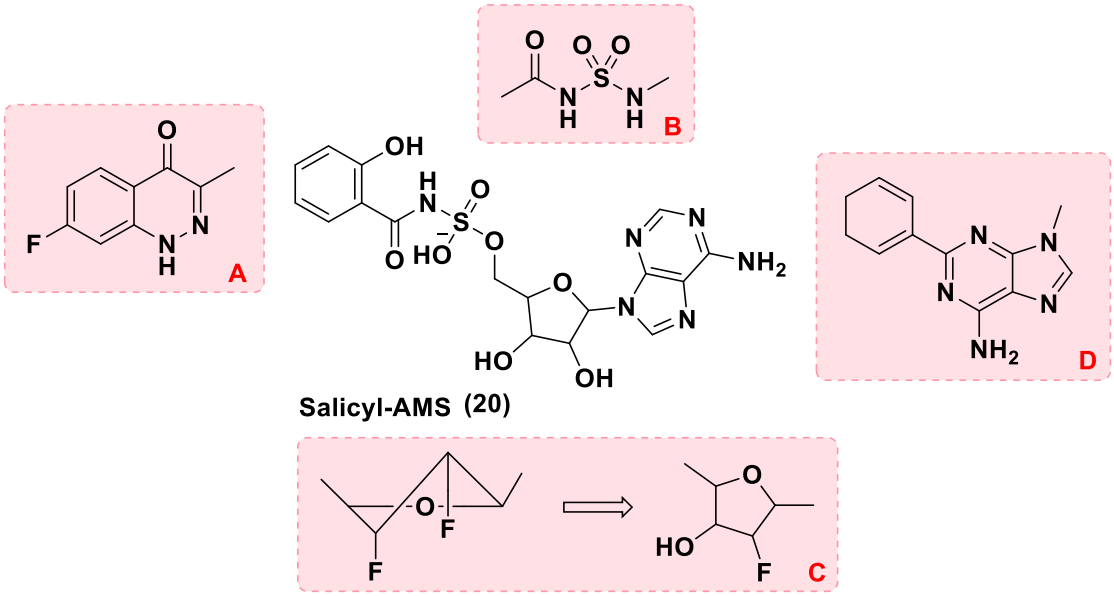

Figure 27. A conclusive summary of the structure-activity relationship on the parent scaffold of Salicyl-AMS **20**, a first-in-class antitubercular agent that targets the first step of the biosynthesis of salicyl-capped siderophores (mycobactins). The main aim behind Salicyl-AMS analogs development was to produce newer candidates with improved PK profile without compromising the antitubercular profile of Salicyl-AMS **20**. Based upon best structural fragmentation analysis, SARs have been elaborated below.

A) Replacement of the *ortho*-hydroxy aromatic group of parent compound **20** with a fluoro-substituted cinnolone unit resulted in analog **50** with potent antitubercular profile (K_i = 11.6 ± 2.4 nM; MIC = 2.3 µM), but most interestingly with a remarkably enhanced PK profile. Oral administration of analog **50** (25 mg/kg) in female Sprague-Dowley rats model indicating 4-time improved in half-life ($t_{1/2}$ = 40 ± 5 i.v., min), 7-fold greater steady state volume of distribution (V_d = 0.57 ± 0.17 i.v.,L.kg^{-1}), and 2-time improved

oral bioavailability (F = 2.1%) compare to lead candidate **20**. Henceforth, we can conclude that replacement of the *ortho*-hydroxy aromatic group with the fluoro-substituted cinnolone moiety may encourage medicinal chemist further analogs development in this direction.

B) Substitution of the sulfamate linker unit with sulfamide bridge **21** led to an increase in overall antitubercular profile (K_i = 3.7 ± 0.6 nM; MIC = 0.19 μM) compared to **20**. Additionally, the PK profile of **21** showed a 3-fold improved oral bioavailability (F = 3.5 ± 0.2 %) and a more than 3-fold higher maximum plasma concentration (C_{max} = 0.70 ± 0.07 μg.mL^{-1}) compared to candidate **20** in a doubly cannulated female Sprague-Dawley rat model.

C) Difluorination of the ribose unit of the nucleosides led to 2′-*endo*, 3′-*exo* conformer **56** with the most promising PK profile in cannulated rat models. The PK profile indicated a 4-fold improved oral bioavailability (F = 5.3 ± 1.3 %) with 15-fold increase in maximum plasma concentration (C_{max} = 5.99 ± 0.56 μg.mL^{-1}) and 25-time greater half-life ($t_{1/2}$ = 267 ± 36 i.v., min) compared to **20** in a doubly cannulated rat model. Despite the most favorable PK profile of analog **56**, this compound showed a significant loss in antitubercular profile (K_i = 139 ± 10 nM; MIC = 37 μM). Analog **73** that contained a mono fluoro-substituted glycosyl moiety, exhibited a significant tubercle bacilli inhibition activity (K_i = 1.6 ± 0.1 nM; MIC = 1.56 μM) with promising PK profile showing a pronounced improvement in oral exposure through a preliminary increase in terminal elimination half-life ($t_{1/2}$ = 121 ± 18 min, i.v.) by blocking P450-mediated metabolism.

D) Incorporation of bulky aryl moieties, *i.e.,* phenyl rings, at the C2 position of the adenine unit of derivative **73** resulted in enhanced MbtA inhibition properties and PK parameters.

IIb. Identification of non-nucleoside MbtA-binding agents:

Targeting mycobactin biosynthesis pathway, and particularly MbtA enzymatic activity, might be a successful strategy in TB drug development. However, from a medicinal chemistry perspective, the majority of Salicyl-AMS derivatives designed so far, although extremely effective against Mtb in iron-depleted conditions, lack drug-like properties. These inhibitors exhibited off-target biological activity and *in vivo* toxicity, displayed poor drug metabolism and pharmacokinetic (DM/PK) profiles, and were likely to undergo the first-pass metabolism before reaching prime infection sites.

To this end, in 2019, the Brucoli group[125] took a different approach for the identification of novel MbtA-binding agents using a combination of whole-cell screening and target-based drug discovery methods. Screening of a diverse compound library, which was selected using standard drug-like parameters, i.e., MW<500, HBD<5, HBA<10, rotatable bonds<10, and PSA<120 Å, against Mtb (H37Rv), yielded a subset of H37Rv-active molecules (~900). After selecting an appropriate MbtA orthologue, e.g., *Msmeg* MbtA (MSMEG_4516), the compounds were tested for their ability to bind to the *Msmeg* MbtA. The binding studies were performed using a robust fluorescence-based thermal shift assay, and Water-Ligand Observed Gradient Spectroscopy (LOGSY), and Saturation Transfer Difference experiments to confirm active-hits and eliminate false positives.

A hit compound 3-(2-((2-nitro-4-(trifluoromethyl)phenyl)-amino)ethyl)-1*H*-indol-5-ol (**78**) (**Figure 28**) was identified from this campaign. The compound showed antitubercular activity against actively replicating Mtb (MIC_{90} H37Rv = 13 μM) and the ability to bind to MbtA. Compound **78** also inhibited the growth of the Koch bacillus in Mtb-infected macrophages (intracellular MIC_{90} = 11 μM in RAW264.7), as

evaluated using a live-cell fluorescence-based screen. Molecular modeling assisted docking of **78** into the proposed binding pocket of MbtA, revealing that **78** and Sal-AMS **20** might occupy different binding orientations in the enzyme.

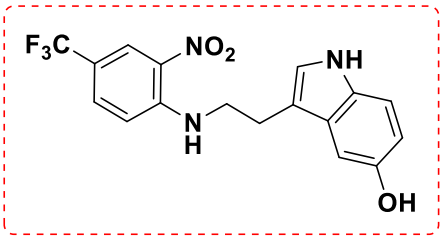

(78)

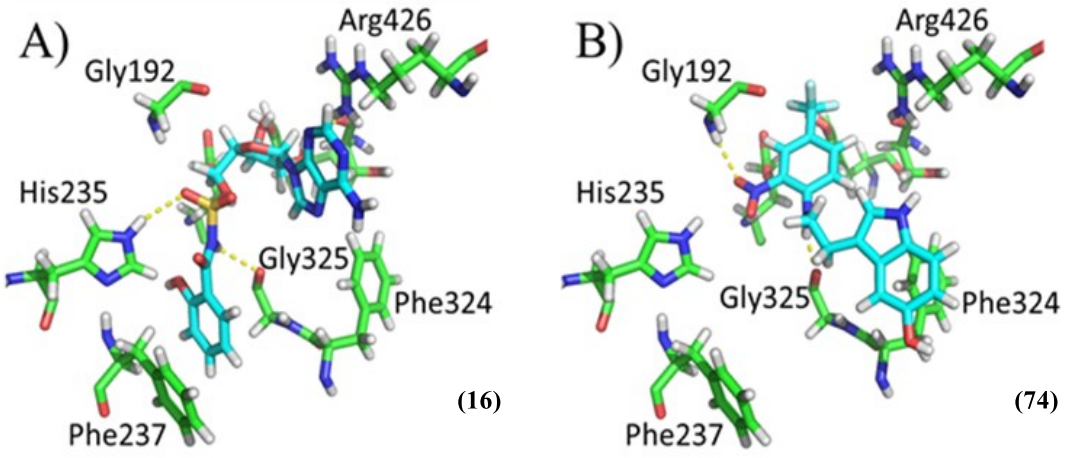

Figure 28. Structures of docked compounds Salicyl-AMS **20** and **78** within the *Msmeg* MbtA active site derived from PDB ID: 5KEI[103]. A) Docked conformation of Salicyl-AMS; B) Docked conformation of compound **78**. Selected residues are shown as green sticks. Yellow dotted lines represent polar interactions. Figures A and B were generated using the PyMOL Molecular Graphics System, Version 1.7 Schrödinger, LLC.

III. Discovery of the C-16 AMS as* MbtM *inhibitor:

Although the leading efforts to target the mycobactins biosynthetic pathway were focused on the development of MbtA and MbtI inhibitors, it is also worth emphasizing the role of the acyl-AMP ligase FadD33 (MbtM) and its potential as a target for novel *ad hoc* inhibitor design to disrupt the Mtb siderophore production.

The synthesis of the core mycobactin scaffold is performed by the enzymatic machinery encoded by the *mbt-1* gene (*mbtA-J*)[93,94] cluster. In contrast, the transfer of the lipophilic aliphatic chain to the ε-amino group of the lysine fragment (directly attached to the 2-hydroxyphenyloxazolidine moiety of the mycobactin) is performed by protein complexes encoded within the *mbt-2* gene (*mbtK-N*)[97] cluster. MbtM is responsible for the activation (adenylation) of the lipophilic acyl chain of mycobactins, which is then loaded onto the phosphopantetheinylated acyl carrier protein MbtL before the final transfer, operated by acyltransferase MbtK to the ε-amino group on the lysine moiety (**Figure 29**).

A study from the Blanchard group[141] demonstrated that FadD33 has a strong affinity for long-chain saturated lipids as substrates and can be inhibited by 5′-*O*-[*N*-(palmitoyl) sulfamoyl] adenosine (**79**, C16-AMS), a structural analog of C12-adenylate (**80**) (**Figure 29**).[142] For this study, MbtM (FadD33) was incubated with several fatty acids of different lengths ranging from C6 - C16 units, including lauric acid, ATP, and C16-AMS. In the assay, significant MbtM-inhibitory activity was observed by the palmitic acid fragment-containing C16-AMS nucleoside.

This might lead to the conclusion that MbtM, a bifunctional enzyme that operates similarly to MbtA, can be a promising drug target for inhibiting mycobactin biosynthesis. The only structural difference between ligands **79** and **20** is represented by the *ortho*-hydroxy aromatic ring of Salicyl-AMS, which is replaced by the linear carbon chain of C-16 palmitic acid.

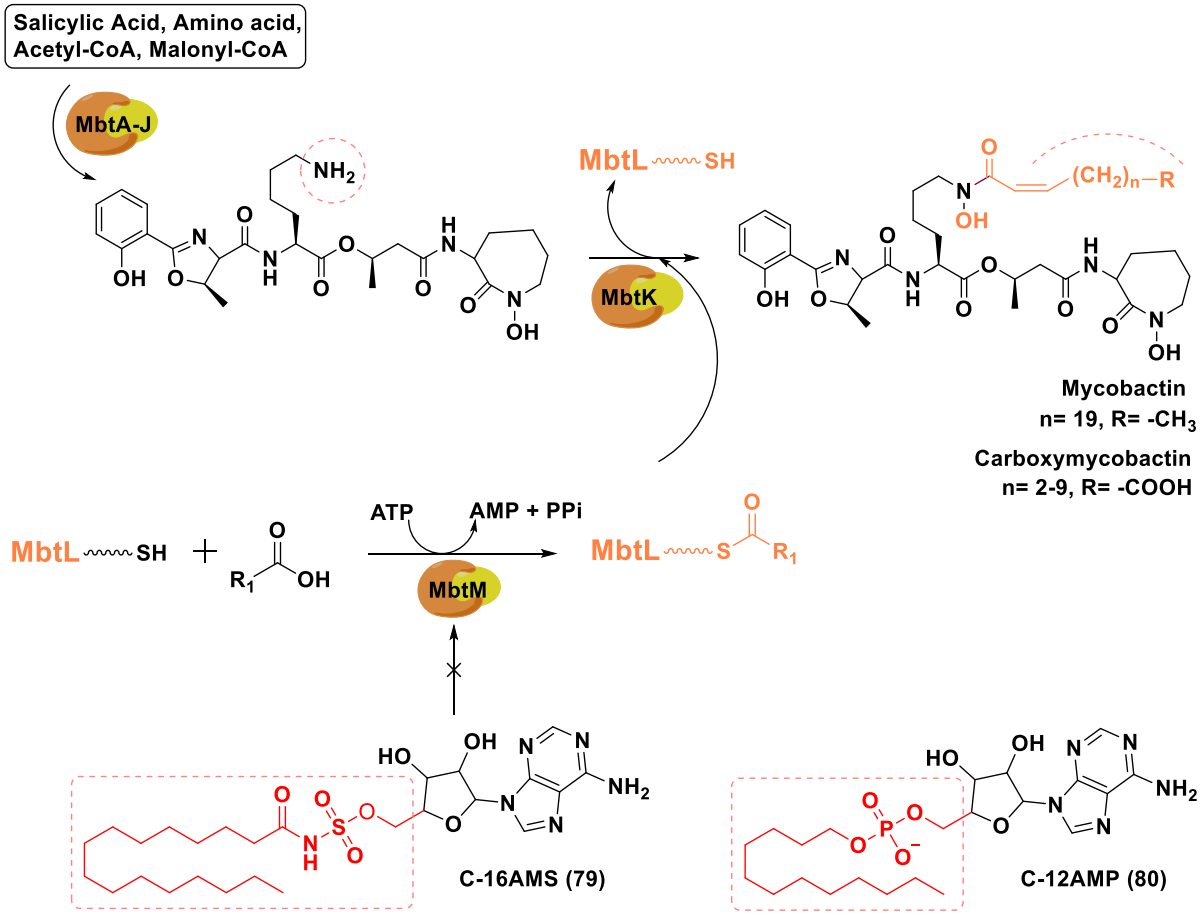

Figure 29. Graphical representation of the significant role of MbtM in the mycobactin biosynthesis pathway. C16-AMS (**79**) was found to inhibit the MbtM enzyme.

IV. PPTase inhibitors' development:

In the complex process of construction of mycobactins, 4'-phosphopantetheinyl transferases (PPTase)[106] play a significant role by translationally modifying carrier proteins (CPs) with the inclusion of a 4′-phosphopantetheine (PPant) moiety. In the mycobacterial NRPS-PKS hybrid systems,[143] the mycobactin framework is constructed by the elongation of a starting monomer followed by the formation of a growing intermediate that is covalently tethered by a carrier protein on to the PPant arm through a thioester linkage.[144] Before receiving the intermediate, the carrier protein must be post-translationally converted from its inactive apo form into its

active holo form. This step is catalyzed by the Mg^{2+} dependent 4′-PPTase that transfers the PPant arm from coenzyme A onto a conserved serine residue of the CP domain through phosphodiester bonds. PPant-chemical intermediate thioester complexes are key elements involved in the secondary metabolites, e.g., mycobactins, chain elongation process in NRPS, PKS, and fatty acid synthetase machineries.[145] PPTase is an attractive antitubercular drug target, and its inhibition can disrupt mycobactin biosynthesis.

In search of potential PPTase inhibitors, Duckworth and Aldrich[146] first developed several potent Sfp 4′-phosphopantetheinyl transferase specific inhibitors. Compound (**81**) was the most promising ligand of the series with a significant PPTase inhibition activity determined by both fluorescence polarization (FP) (K_i = 0.180 ± 0.01μM) and isothermal titration calorimetry (ITC) (K_i = 0.609 ± 0.088μM) assays. Two more ligands, sanguinarine chloride (**82** and **83**), were also tested in this work. However, **82** displayed inferior activity in the FP and ITC assays. Further to this, Vickery et al.[147] solved the X-ray crystal structure of Sfp-type PPTases from two of the most prevalent mycobacterial species, *M. tuberculosis* and *M. ulcerans,* and identified specific PPTase inhibitors in their work. Among the small library of inhibitors evaluated in the study, ligand **82** was the most potent inhibitor against the target proteins with IC_{50} values ranging from 4.9 ± 0.2 μM to 22 ± 2 μM. Rohilla et al.[148] carried out a docking and cheminformatics study to identify some potent PPTase inhibitors using Autodock 4.2 and Glide platforms. The ligand PS-40 (NSC-328398, **83**) emerged as the most potent inhibitor with IC_{50} and MIC_{90} values of 0.25 μg/ml and 10 μg/ml, respectively. Negligible cytotoxicity was observed against three mammalian cell lines with the selectivity index greater than 10. Grunewald et al.[149] prepared a unique antibody-drug conjugate system (ADCs, **84**) utilizing 11- and 12-mer aminoacidic substrates of phosphopantetheinyl transferase as warheads to be linked to the antibody. Using Sfp-PPTase, 63 sites could be efficiently labeled with an auristatin toxin, resulting in 95 homogeneous ADCs. An 11- and a 12-mer PPTase substrate

sequences were inserted at the 110 constant region loop positions of trastuzumab IgG. Insertion of 11– and12-mer peptide tags impacted the thermal stability and PK profiles. The peptide tag between residues 118-215 was labeled as CH1 domain, where residues 228-340 and residues 341-447 spacing indicated the CH2 and CH3 domains, respectively. The melting temperature (T_m) values of antibodies with insertions in the CH1 and CH3 domains were on average 1.4 – 4.2 °C lower than that of trastuzumab (T_m = 69.7°C). In the case of the CH2 domain, the average value of the construct was 13.3°C indicating that the insertion site strongly modulated thermal stability irrespective of the drug molecule. The ADCs labeled in the CH2 domain displayed an excellent PK profile due to the faster clearance from the circulation with negligible drug loss. This approach resulted in a site-specific drug delivery system with considerably better PK profile and an interesting *in vitro*/*in vivo* profile (**Figure 30**).

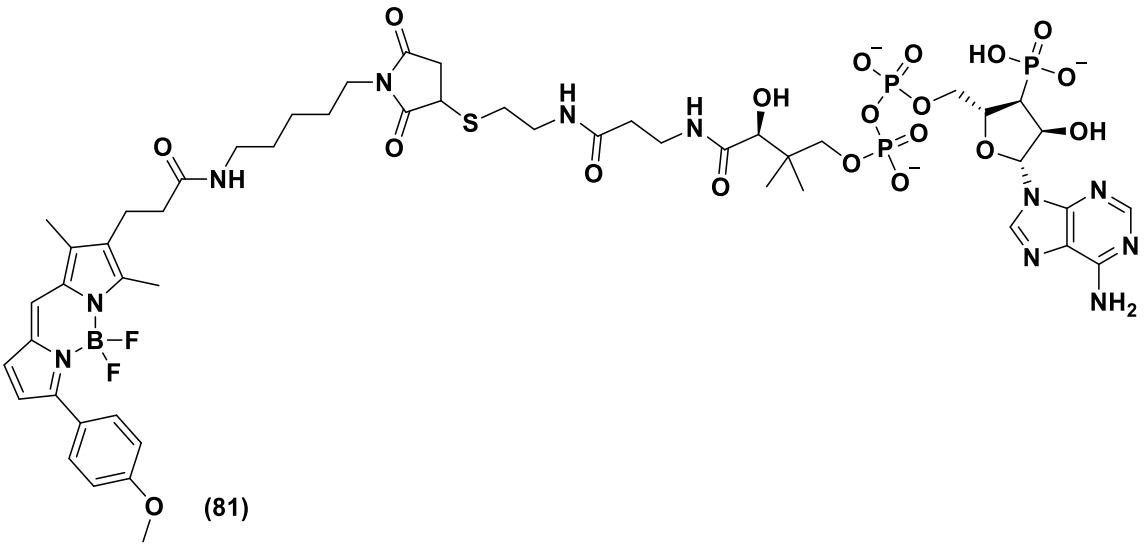

(81)

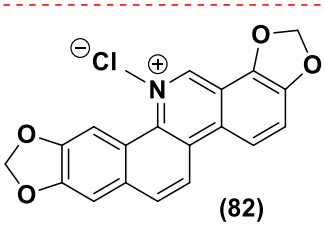

(82)

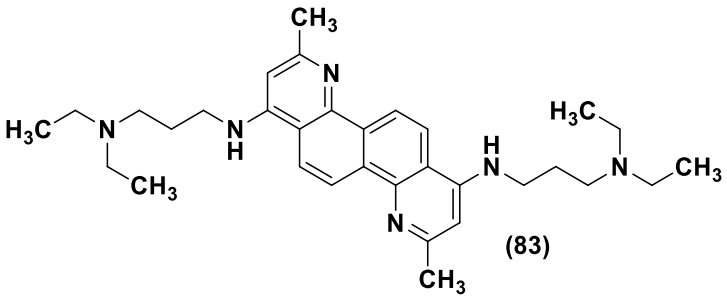

(83)

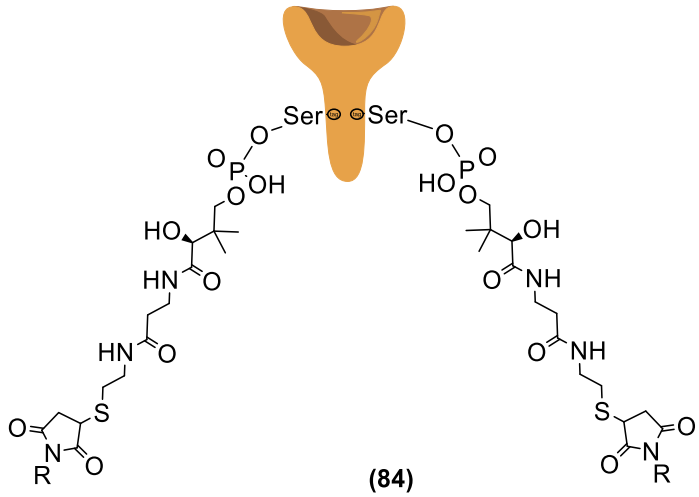

(84)

Figure 30. Chemical structures of the PPTase inhibitors (**81**-**83**) and representation of antibody-drug conjugate system (ADC) **84** utilizing aminoacidic substrates of phosphopantetheinyl transferase as a pay-load warhead.

Nucleoside analogs are designed to mimic endogenous substrates and inhibit the activity of target enzymes involved in the mycobactin biosynthesis. A series of nonspecific mycobactin biosynthesis inhibitors and non-conventional antitubercular drug delivery systems proposed to disrupt mycobacterial siderophore synthesis have been reported below.

V. Nonspecific Mycobactin Biosynthesis Inhibitors:

Several analogs structurally related to the mycobactins were designed, synthesized, and evaluated against Mtb under iron-deprived (GAST) and iron-rich conditions (GAST-Fe) for a comparative assessment. The primary assumption behind this synthetic strategy was that mycobactin-mimicking compounds with structural features of mycobacterial siderophores might disrupt the ferri-mycobactin transport systems across membranes, inhibit enzymes related to siderophores biosynthesis, and arrest bacterial growth under iron-deprived conditions. Three classes of mycobactin analogs have been designed so far based on this hypothesis. Their molecular characteristics and antitubercular activity are described in the next section.

A. Pyrazoline analogs:

In 2008 Stirrett et al.[150] synthesized a library of small molecules with structural similarities to the mycobactins framework and evaluated them against Mtb. Their basic structural scaffold comprised the 3,5-diaryl-1-carbothioamide–pyrazoline motif, which resembled

the hydroxyphenyl-oxazoline unit of the mycobactin and carboxymycobactin siderophores. The compounds were not target specific and were evaluated for their ability to arrest the growth of Mtb in both iron-deficient and iron-rich media and to inhibit a salicylation enzyme targeted by Salicyl-AMS **20**. The bactericidal compound (**85**) displayed a very high antitubercular activity in the series, with IC_{50} and MIC_{90} values of 8 and 21 μM, respectively, in iron-deprived conditions. The analog **85** showed no cytotoxicity against HeLa cells (CD_{50} = 398 μM), and the candidate was not active against Mtb (MIC_{90} = 333 μM) in iron-rich media GASTD+Fe, thus indicating its involvement in mycobactins system functionalities with a remarkable selectivity index (SI_{Mtb} = $IC_{50GAST-D}$/ IC_{50GAST}) value of 15. The scaffold of analog **85** provided a promising platform for lead design against conditionally essential targets (CETs) and for exploring the mycobactin synthetic pathway. In continuation of this work, in 2011, Ferreas et al.[151] designed two libraries of mycobactin analogs containing the diaryl-substituted pyrazoline (DAP) and (2*E)*-2-benzylidene-*N*-hydroxyhydrazine carboxamide (BHHC)-based scaffolds. The DAP and BHHC derivatives were evaluated against Mtb and *Yersinia pestis*. Among the active DAP derivatives, compounds (**86**) and (**87**) were the most potent against Mtb (IC_{50} = 4 - 7μM, MIC = 16 μM). Among the BHHC derivatives series with defined IC_{50} and MIC values, (**88**) and (**89**) were the most active against Mtb (IC_{50} = 2-4μM, MIC = 6-10 μM). These two compounds displayed no significant cytotoxicity in mammalian cells at their respective MIC values. However, the majority of active compounds exhibited similar antitubercular activity in both iron-depleted (GAST) and iron-replete (GAST+Fe) media, suggesting that the compounds' targets might be linked to mycobacterial processes essential in both low and high iron conditions (**Figure 31**).

B. Oxazole and Oxazoline analogs:

Moraski et al.[152] in 2010 also designed a >100-member library of mycobactin analogs utilizing the oxazoline and oxazole scaffolds to mimic the hydroxyphenyl-oxazoline motif of the Mtb siderophores. The study rationale was based on previous findings related to ND-005859[153] (**90**), a non-iron binding, dibenzyl-protected oxazoline molecule, which is a precursor in the synthesis of mycobactin S and T (**Figure 5**). Compound **90** exhibited a remarkable antitubercular activity (MIC = 7.7 μM) and was non-cytotoxic against Vero cells (IC_{50} = >128 μM). Interestingly, after deprotection of the benzyl groups, the resulting ND-005862 analog, which possessed iron-chelating properties, lost the antitubercular activity of the parent compound completely. From this observation, the group explored the SAR around hit compound **90** and synthesized easily accessible derivatives bearing the benzyl ester unit that were tested *in vitro* against Mtb in iron-deprived conditions and *in vivo* to assess toxicity using BALB/c mice.

A large number of these oxazole derivatives showed significant antitubercular activity and, in particular, compound (**91**), which had a MIC value of <0.5 μM against replicating H37Rv and was not cytotoxic in Vero cells (IC_{50} = 121 μM). However, the metabolic instability of the benzyl esters prevented their use as orally active pre-clinical candidates (**Figure 31**).

C. Chromane derivatives:

In 2012,[154] Veerepalli et al. designed and synthesized chromeno[4,3-*d*]benzimidazo [1,2-*a*] pyrimidine analogs as siderophore inhibitors. The compounds contained a 2-phenyl-3,4-dihydro-2*H*-chromene (flavan) skeleton that mimicked the 2-hydroxyphenyl-oxazoline moiety of mycobactins. Among the designed derivatives, analogs that contained chloro-substitutions on the aromatic ring directly attached to the benzopyran scaffold displayed the highest potency with better inhibitory selectivity toward Mtb grown in an iron-deplete medium. The benzopyran moiety has a chloro-phenyl substituent (**92**) showed significant

activity against Mtb (H37Rv) in iron-deficient medium with IC_{50} values of 0.35 ± 0.27 μM, whereas, in iron-rich conditions, the derivatives showed poor antimycobacterial activity (IC_{50} = 70 ± 3.75μM) (**Figure 31**).

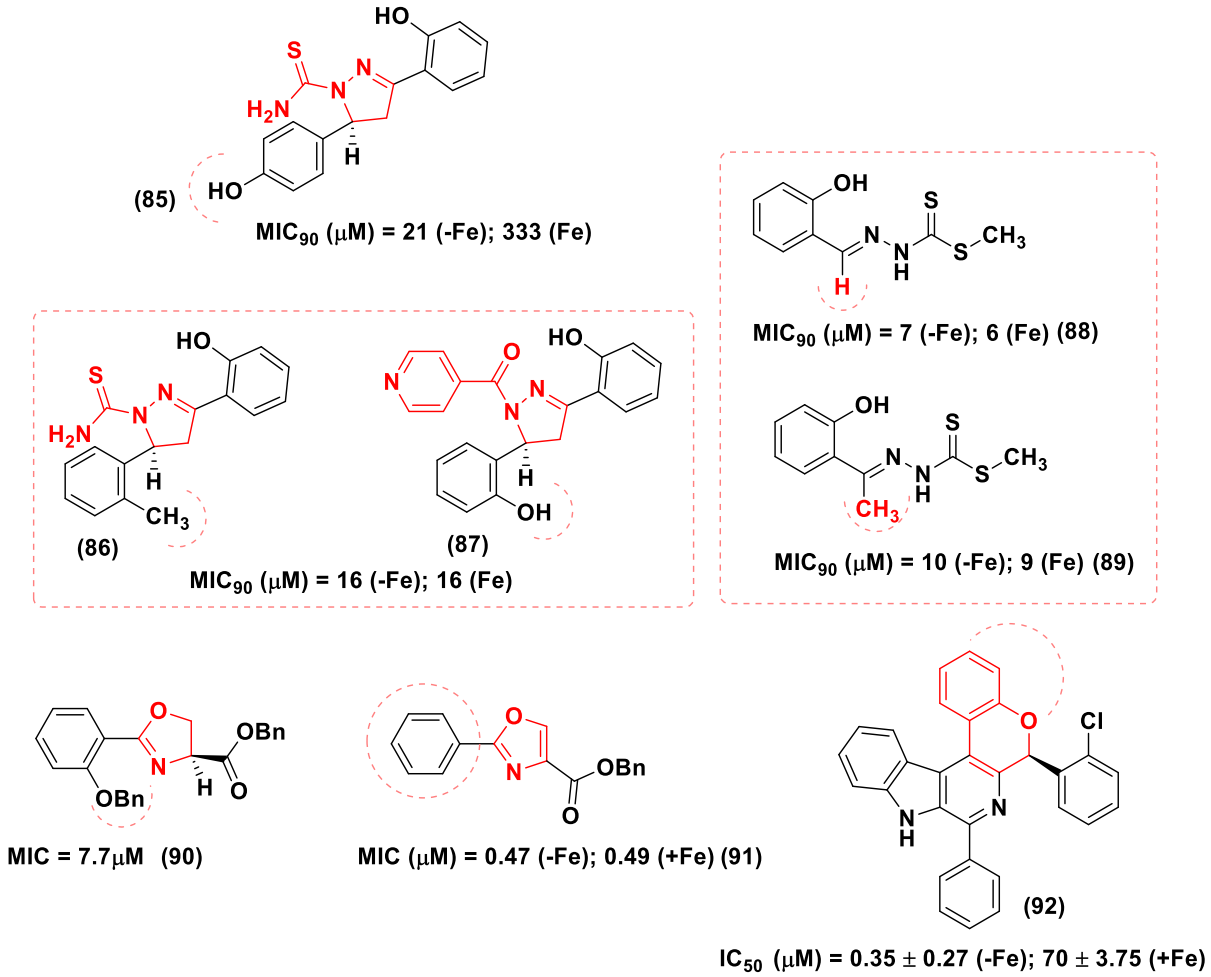

Figure 31. Nonspecific mycobactin inhibitors **85-92** showing significant antitubercular activity against Mtb cultured in iron-rich media. Compounds **86 - 89** whose structures included mycobactin-resembling units, exhibited anti-TB activity irrespectively of the iron content environment. These agents were not designed with a specific enzyme as the target. However, derivatives **90** and **91** that showed remarkable anti-TB activity in iron-deficient conditions might impair siderophore-related transport systems and enzymatic processes by virtue of their

molecular frameworks, which incorporated structural features resembling portions of the mycobacterial siderophores scaffolds, *i.e.,* the salicyl-capped oxazoline component.

Canonical medicinal chemistry strategies were adopted to target the Mtb siderophores systems with Sal-AMS nucleoside analogs and mycobactin-mimicking molecules. However, an alternative approach, which involved the synthesis of heterodimeric mycobactin-conjugated drug delivery system, has also been adopted to disrupt iron metabolism in mycobacteria. This unique drug delivery system was successfully employed to impair iron chelation and -uptake mechanisms in drug-sensitive and MDR Mtb strains.

VI. Alternative heterodimeric antitubercular drug delivery systems. The Trojan Horse Approach:

The heterodimeric hybridization represents an advanced and inventive molecular technique that involves the covalent linkage of two antibiotic pharmacophores, with a known mechanism of action, to form one molecule that might inhibit different targets within a bacterial cell[155]. In addition to this, the molecular heterodimerization approach can be coupled with the 'Trojan horse' strategy to introduce the antibiotic of interest into the pathogen cell via siderophore receptors on the bacterial outer membrane. In this instance, the siderophores, *i.e.,* mycobactins covalently linked to an antimicrobial agent, are used as vectors to transport antibiotics within the cell. This is a well-documented approach and has even been developed by various bacteria to kill other microorganisms.[156]

In 2011[157], Miller and co-workers used the 'Trojan horse' approach to design the mycobactin-artemisinin heterodimer conjugate (**93**), which exhibited remarkable activity against both Mtb (H37Rv) and the malaria plasmodium (**Figure 33**). The iron-chelating component (*i.e.*, mycobactin) of hybrid molecule **93** activates the antibiotic activity of the artemisinin moiety,

which requires iron to reduce, and then cleaves its peroxide bond. Therefore, the reduction of ferric (Fe^{3+}) to ferrous (Fe^{2+}) iron carried within the hybrid scaffold **93** might lead to Fenton radical reactions with the formation of reactive oxygen species that negatively impact the survival of the mycobacteria. The mycobactin-artemisinin conjugate **93** improved the antibacterial and anti-parasitic activity of artemisinin, which is not active against Mtb as a single agent and exhibited significant antitubercular activity against H37Rv (MIC = 0.39 μg/ml), MDR- (MIC = 0.16-1.25 μg/ml) and XDR-strains (MIC = 0.078-0.625 μg/ml) of Mtb. In 2012,[158] further studies by Miller's group reported the synthesis of three mycobactin T analogs (**94**-**96**) bearing a mixture of *tert*-butyloxycarbonyl (Boc) and acetate (Ac) protecting groups. Compound **94** contained an additional maleimide unit, which was linked through a valerate residue to a newly installed C4 amino group in the aromatic ring (salicyl-capped unit) of the mycobactin core. Derivatives **94-96** were more potent than **93** and showed excellent antitubercular activity with MIC_{90} values ranging from 0.02 – 0.88 μM against Mtb H37Rv strains cultured in 7H12 and GAS media. The compounds were selective toward Mtb with no inhibitory effects against a panel of Gram-positive and Gram-negative (**Figure 32**).

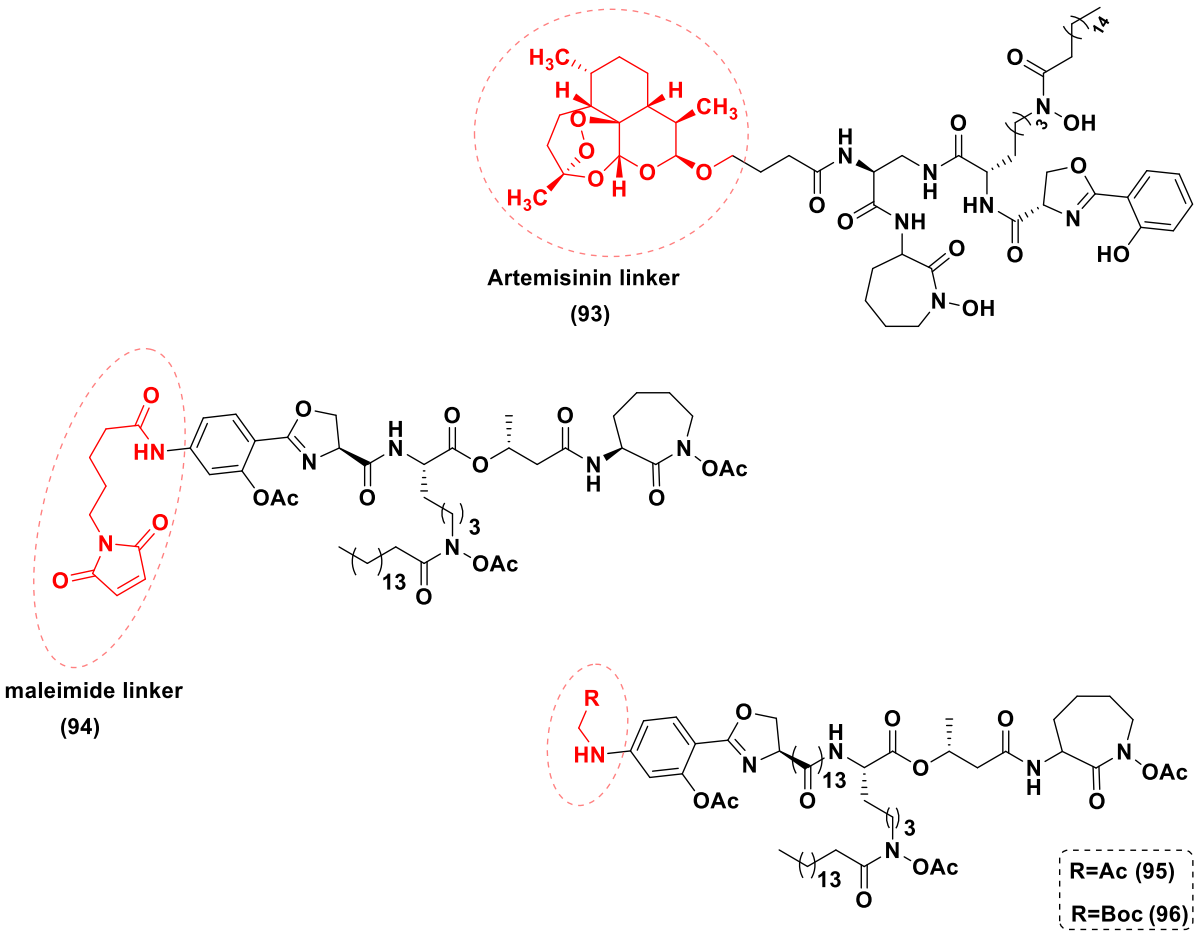

Figure 32. Hybrid siderophore−drug conjugates developed by Miller et al. The mycobactin-artemisinin (in red) heterodimer **93** exhibited remarkable anti-malarial and anti-tuberculosis activity. Siderophore-maleimide conjugates **94-96**, which synthesized through a thiol-maleimide reactive system, displayed improved antitubercular activity compared to **93**.

Conclusion:

Despite significant progress in clinical drug candidate development for TB treatment in the last 10–15 years, TB continues to be a major health burden in developing countries. The hunt for drug candidates that inhibits novel targets remains to be a pressing area of research. Studies toward a deeper understanding of Mtb biology have resulted in some progress, uncovering new

therapeutic targets. Notably, in this review, we have shed light on the mycobactin biosynthesis complex responsible for the essential iron transportation in Mtb. Interference with this conditionally essential pathway could be an attractive strategy for discovering antitubercular therapy. Iron is an ideal candidate for a redox catalyst in several cellular processes due to its ability to switch between two oxidation states. It is an essential nutrient for most microbes.[159,160] It has been observed that the impairment of mycobactin biosynthesis and iron acquisition process directly affects mycobacterial virulence and its survival in the host.[107,86] In addition, the absence of this pathway in human hosts minimizes the risk posed by off-target effects. Any resistance mechanisms in these targets are not known yet.

Structure-based rational design of MbtI and MbtA inhibitors have thus far shown promising results. In regard to salicylate synthase (MbtI) inhibitors, the development of TS inhibitors was the first stepping stone. Further development in this direction did not yield any significant candidate except C2, C3-hydroxybenzoate analog **7**, with a K_i value of 11 μM. High throughput virtual screening led to the identification of small molecule heterocyclic inhibitor **12** with an IC_{50} value of 5.89 μM. Thereafter, research in furan analogs development produced candidate **18** (K_i = 3.1 ± 1.0 μM, IC_{50} = 6.3 ± 0.9 μM) as the most promising MbtI inhibitor up-to-date. For Salicyl-AMP ligase (MbtA) inhibitors, bioisosteric replacement of phosphate in the linker region of Salicyl-AMP, **19**, resulted in a potent Salicyl-AMP ligase inhibitor, Salicyl-AMS **20**. Further modifications were attempted in the linker region, salicylic aromatic ring, sugar moiety, and nucleobase unit to improve the nucleoside (**20**) weak PK profile. The replacement of the ortho-hydroxy functional group on the salicylic ring with 7-fluorocinnolone resulted in analog **50** and insertion of a fluorinated ribose moiety and a C-2 phenyl substituent in the adenine unit led to derivative **73** that showed an improved the PK profile compared to the parent compound (**20**). Moreover, the discovery of the ligand **78** prompted further research toward small

inhibitors development as potential MbtA inhibitors. To date, C16-AMS (**79**) is the only candidate identified as an MbtM inhibitor. In the case of potent MbtI inhibitor **18** and MbtM inhibitor **79**, a PK profile has not yet been generated, and further studies, including PK profile development, are still required for nonspecific mycobactin biosynthesis inhibitors.

Inhibitors for other enzymes in the mycobactin biosynthetic pathway are yet to be explored. Structure-based inhibitor design is a feasible approach. However, the real challenge is to establish a *proof-of-concept* that requires the respective enzymes to be recombinantly expressed. It is also necessary to establish *proof-of-concept* in an infected animal model. The design of an enzyme inhibition assay with the multimodular enzymes is another critical bottleneck. Success in continuous tailoring multimodular NRPS proteins to synthesize heterocyclic ring systems and newer antibiotics provides hope that these techniques may offer enzyme inhibition study platforms for unexplored enzymes in the mycobactin biosynthetic pathway.[161,162]

Small molecules containing heterocycles, such as pyrazoles, oxazoles, and coumarins mimicking the structure of 2-hydroxyphenyl-oxazoline have been designed previously. These compounds inhibited the growth of Mtb under iron-deprived conditions. However, no attempt was made to date to identify the target proteins. Further research in this direction is recommended to expedite antitubercular drug discovery to cope with the rising concern related to resistant strains. In continuation with our previous efforts,[125, 150, 151] we are currently in the process of developing target-based inhibitors with favorable biological and PK profiles.

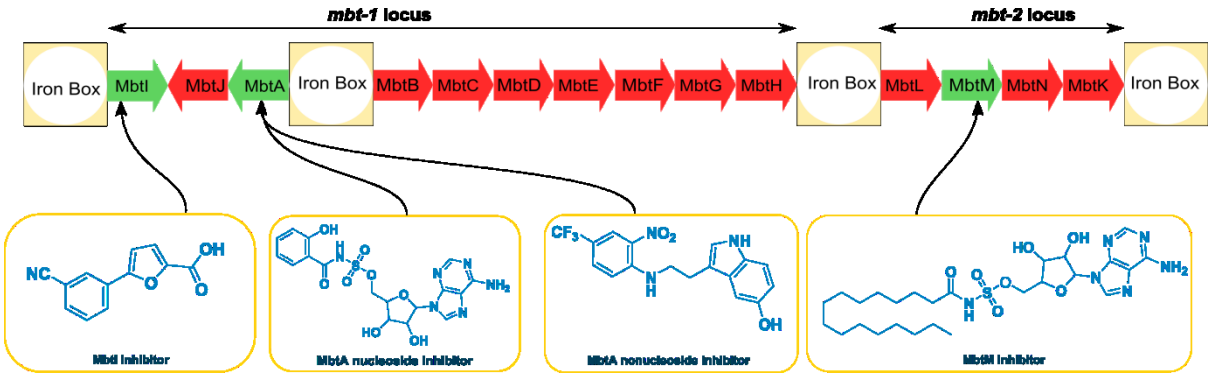

Figure 33. The *mbt* gene cluster provides a golden opportunity to accelerate enzyme-based antitubercular drug discovery. Enzymatic targets MbtA, MbtI, and MbtM already have shown to be promising antitubercular drug targets for novel TB drug design and development.

The significant role of the conditionally essential 14 enzymes of the *mbt* gene cluster may encourage medicinal chemists to develop new lead-compounds with a novel mode of action to counter the drug-resistant strains of the tubercle bacilli **(Figure 33)**. At the same time, the biological and biochemical vulnerabilities of each enzymatic target produced by the *mbt* gene cluster must be considered for the identification of the most chemically tractable NRPS-PKS protein targets of Mbt. Understanding endogenous interactions between prospective drugs with their therapeutic targets might pave the way for the development and implementation of novel and innovative approaches to antibiotic discovery.

Acknowledgments:

Authors acknowledge the Department of Science and Technology- Science and Engineering Research Board (DST-SERB File. No: EMR/2016/000675 dt. 05/08/2016) and a Global Challenges Research Fund to SB for the financial support in building a UK-India capacity for tackling antimicrobial drug resistance in tuberculosis. MS is a Newton-Bhabha International Fellow (BT/IN/NBPP/MS/20/2019-20 dt. 04/03/2020)

Abbreviations Used:

atpE, ATPase epsilon; CET, Conditionally Essential Target; CPs, carrier proteins; CUEs, chorismate-utilizing enzymes; DAP, Diaryl-substituted pyrazoline; DHFR, dihydrofolate reductase; DM/PK, drug metabolism/pharmacokinetics; DosR, dormancy survival regulon; FP, fluorescence polarization; GAST medium, glycerol-alanine-salts medium; ITC, isothermal titration calorimetry; KatG, catalase-peroxidase; MDR, multi-drug-resistant; Mtb, *Mycobacterium tuberculosis*; NRPS, nonribosomal peptides synthetases; PDB, protein data bank; PDIM, phthiocerol dimycoceresates; PKS, polyketide synthase; pncA, pyrazinamidase/nicotinamidase; PPTase, phosphopantetheinyl transferase; Rec, receptor protein; RNIs, reactive nitrogen intermediates; Rpf, resuscitation promoting factor; rpsL, ribosomal protein S12; rrs, ribosomal RNA; TDR, Total drug-resistant; *thyA,* thymidylate synthase; TS, Transition State; WHO, World Health Organization; XDR, extensively drug-resistant;

Author Biographies

Mousumi Shyam is a doctoral research scholar at the Department of Pharmaceutical Sciences and Technology, Birla Institute of Technology, Mesra (India). Her research area includes siderophore targeting antitubercular drug designing and development to tackle the global burden of drug-resistant TB. She was a Junior Research Fellow from January 2017-January 2019 period and Senior Research Fellow for January 2019-December 2019 duration under DST-SERB funded project (File. No: EMR/2016/000675 dt. 05/08/2016). She was a Sakura Science Exchange fellow in 2019 at the University of Miyazaki, Japan funded by Japan Science and Technology. Currently, she has received Newton-Bhabha Research Fellowship (BT/IN/NBPP/MS/20/2019-20 dt. 04/03/2020) to work under the supervision of Professor Sanjib Bhakta at Birkbeck, University of London.

Deepak Shilkar received his Bachelor of Pharmacy degree in 2016 from Goa University (India) and an M.Sc. in Drug Discovery in 2018 from UCL School of Pharmacy, London. Currently, he is working as a Junior Research Fellow at Birla Institute of Technology, Mesra (India). He is interested in studying tropical infectious diseases as well as pathogenic viruses affecting humans and animals.

Harshita Verma has completed her Master of Science (Hons.) Biological Sciences from Birla Institute of Technology and Science, Pilani, India. She has completed her Master thesis in CSIR-National Chemical Laboratory, India. Her research interest lies in antimicrobial resistance and exploring new therapeutics to combat it. She has completed projects in *Plasmodium vivax* and *Toxoplasma gondii* and has developed skills in molecular biology and microbiology. Currently, she is pursuing an MRes Global Infectious Diseases research intense program at Birkbeck, University of London where she is investigating mycobactin biosynthesis in *Mycobacterium tuberculosis* under the guidance of Professor Sanjib Bhakta.

Dr Abhimanyu Dev received his M. Pharm in Pharmaceutical Biotechnology and Ph. D. on

the topic “Antigen delivery and oral vaccination” from BIT Mesra. He is currently working as an Assistant Professor in the Department of Pharmaceutical Science and Technology, Birla Institute of Technology, Mesra (India). He has been a recipient of 5 sponsored research grants including one from DST Nanomission. He is a co-investigator on the DST grant on Phenyloxazoline Synthetase Inhibitors as Antitubercular Agents. His research interests include anticancer drug delivery systems, theranostics, and anti-TB research.

Professor Barij Nayan Sinha received his M. Pharm from Banaras Hindu University (India) and PhD from Birla Institute of Technology, Mesra (India). He is currently working as a Professor at the Department of Pharmaceutical Sciences and Technology, BIT Mesra. He has been the Principal and Co-investigator on 10+ funded projects including three international collaborations. Two (Indo-German (DBT-BMBF) Program) on topics of Antiviral Agents for the treatment of Chikungunya and Dengue viral infections and another was UGC-UKIERI in the area of Anticancer Agents. His research interests include antiviral and anticancer drug discovery and natural product chemistry using modern analytical techniques.

Dr Federico Brucoli has a degree in Pharmacy from the University of Palermo, Italy, and a PhD in medicinal chemistry from the UCL School of Pharmacy, London. Dr Brucoli was a Maplethorpe fellow at UCL. After being appointed as a chemistry lecturer at the University of the West of Scotland, Scotland, UK, he moved to Leicester, UK, where is currently a senior lecturer in medicinal chemistry at the School of Pharmacy, De Montfort University. His research interests focus on antibacterial and cancer chemotherapy, and the study of natural products as templates for future drug design. Recent efforts have been directed toward the identification of new therapeutic drug leads to combat tuberculosis, a serious infectious disease caused by the slow-growing Mycobacterium tuberculosis bacterium.

Professor Sanjib Bhakta has a PhD in Molecular Microbiology & Biochemistry from Bose Institute (India). He joined the Oxford University Division of Medical Sciences as an Oxford

University Innovation Senior Research Scholar and shortly after he was awarded a Wellcome Trust international post-doctoral fellowship. He graduated from The Queen's College, University of Oxford completing a second doctoral degree (DPhil in Pharmacology) and received a "Sir William Paton Prize" from the Oxford University Division of Medicine. He is currently a full-Professor of Molecular Microbiology and Biochemistry, Dean (Internationalization and Partnerships) and Program Director of MRes Global Infectious Diseases at the Institute of Structural and Molecular Biology of Birkbeck, University of London and UCL. His research is focused on developing novel therapeutics as well as drug repurposing.

Dr Venkatesan Jayaprakash received his M. Pharm degree in Pharmaceutical Chemistry from Banaras Hindu University, Varanasi (India) and his PhD in Pharmacy from Birla Institute of Technology, Mesra (India). He is currently working as an Associate Professor at Birla Institute of Technology, Mesra (India). His research interests focus on antibacterial and antiviral drug discovery using in-silico and structure-based drug design approaches. He is a recipient of several sponsored research grants on infectious disease research and currently has active collaborations with researchers in Europe and North America. He is currently leading efforts for the development of Phenyloxazoline Synthetase inhibitors as Antitubercular Agents as the principal investigator on a DST grant and has long been involved in the development of anti-TB therapeutics by exploring novel targets.

References:

1. World Health Organization. *The WHO Global Task Force on TB Impact Measurement*; https://www.who.int/tb/areas-of-work/monitoring-evaluation/impact_measurement_taskforce/en/ (accessed Nov 7, 2019). World Health Organization: **2019**.
2. Daniel, T. M.; Bates, J. H.; Downes, K. A. History of tuberculosis. *Tuberculosis: pathogenesis, protection, and control.* **1994**, 13-24.
3. Zumla, A.; Squire, S. B.; Chintu, C.; Grange, J. M. The tuberculosis pandemic: implications for health in the tropics. *Trans. R. Soc. Trop. Med. Hyg.* **1999**, *93*, 113-117.
4. Russell, D. G.; Cardona, P. J.; Kim, M. J.; Allain, S.; Altare, F. Foamy macrophages and the progression of the human tuberculosis granuloma. *Nat. Immunol.* **2009**, *10*, 943-948.
5. Harding, E. WHO global progress report on tuberculosis elimination. *Lancet Respir. Med.* **2020**, *8*, 19.
6. Herzog, H. History of tuberculosis. *Respiration* **1998**, *65*, 5-15.
7. Moris, G.; Garcia-Monco, J. C. The challenge of drug-induced aseptic meningitis. *Arch. Intern. Med.* **1999**, *159*, 1185-1194.
8. Gengenbacher, M.; Kaufmann, S. H. *Mycobacterium tuberculosis*: success through dormancy. *FEMS Microbiol. Rev.* **2012**, *36*, 514-532.
9. Gupta, A.; Kaul, A.; Tsolaki, A. G.; Kishore, U.; Bhakta, S. *Mycobacterium tuberculosis*: immune evasion, latency and reactivation. *Immunobiology* **2012**, *217*, 363-374.
10. Russell-Goldman, E.; Xu, J.; Wang, X.; Chan, J.; Tufariello, J. M. A *Mycobacterium tuberculosis* Rpf double-knockout strain exhibits profound defects in reactivation from chronic tuberculosis and innate immunity phenotypes. *Infect. Immun.* **2008**, *76*, 4269-4281.
11. Kana, B. D.; Mizrahi, V. Resuscitation-promoting factors as lytic enzymes for bacterial growth and signaling. *FEMS Immunol. Med. Microbiol.* **2010**, *58*, 39-50.

12. Leistikow, R. L.; Morton, R. A.; Bartek, I. L.; Frimpong, I.; Wagner, K.; Voskuil, M. I. The *Mycobacterium tuberculosis* DosR regulon assists in metabolic homeostasis and enables rapid recovery from nonrespiring dormancy. *J. Bacteriol.* **2010**, *192*, 1662-1670.
13. Boon, C.; Dick, T. How *Mycobacterium tuberculosis* goes to sleep: the dormancy survival regulator DosR a decade later. *Future Microbiol.* **2012**, *7*, 513-518.
14. Arroyo, L.; Marín, D.; Franken, K. L.; Ottenhoff, T. H.; Barrera, L. F. Potential of DosR and Rpf antigens from *Mycobacterium tuberculosis* to discriminate between latent and active tuberculosis in a tuberculosis endemic population of Medellin Colombia. *BMC Infect. Dis.* **2018**, *18*, 26.
15. Hett, E. C.; Rubin, E. J. Bacterial growth and cell division: a mycobacterial perspective. *Microbiol. Mol. Biol. Rev.* **2008**, *72*, 126-156.
16. Barry, C. E.; Boshoff, H. I.; Dartois, V.; Dick, T.; Ehrt, S.; Flynn, J.; Schnappinger, D.; Wilkinson, R. J.; Young, D. The spectrum of latent tuberculosis: rethinking the biology and intervention strategies. *Nat. Rev. Microbiol.* **2009**, *7*, 845-855.
17. Unissa, A. N., Rational drug designing strategies for *Mycobacterium tuberculosis*. *Int. J. Pharma. Biol. Sci.* **2011***, 1,* 534–555.
18. Pfuetze, K. H.; Pyle, M. M.; Hinshaw, H. C.; Feldman, W. H. The first clinical trial of streptomycin in human tuberculosis. *Am. Rev. Tuberc.* **1955***, 71*, 752-754.
19. Wilson, J.; Kelkar, P.; Frigas, E., Para-aminosalicylic acid (PAS) desensitization review in a case of multidrug-resistant pulmonary tuberculosis. *Int. J. Tuberc. Lung. Dis.* **2003**, *7*, 493-497.
20. Selikoff, I. J.; Robitzek, E. H.; Ornstein, G. G. Treatment of pulmonary tuberculosis with hydrazide derivatives of isonicotinic acid. *J. Am. Med. Assoc.* **1952**, *150*, 973-980.
21. Daniel, T. M., Rifampin—a major new chemotherapeutic agent for the treatment of tuberculosis. *N. Engl. J. Med.* **1969**, *280*, 615-616.

22. Lewis, K. Platforms for antibiotic discovery. *Nat. Rev. Drug. Discov.* **2013**, *12*, 371-387.
23. World Health Organization. Guidelines for treatment of drug-susceptible tuberculosis and patient care. 2017 Update; https://apps.who.int/iris/handle/10665/255052 (accessed Aug 5, 2019) World Health Organization: **2017**.
24. Gilpin, C.; Korobitsyn, A.; Migliori, G. B.; Raviglione, M. C.; Weyer, K., The world health organization standards for tuberculosis care and management. *Eur. Respir. J.* **2018**, *51*, 1800098.
25. Uttley, A. H.; Pozniak, A. Resurgence of tuberculosis. *J. Hosp. Infect.* **1993**, *23*, 249-253.
26. Nakajima, H. Tuberculosis: a global emergency. *World Health* **1993**, *46*, 3-3.
27. Osborne, R. First novel anti-tuberculosis drug in 40 years. *Nat. Biotechnol.* **2013**, *31*, 89-91.
28. World Health Organization. The use of bedaquiline in the treatment of multidrug-resistant tuberculosis: interim policy guidance. https://www.who.int/tb/publications/mdrtb-treatment-guideline/en/ (accessed Nov 11, 2019) World Health Organization: **2013**.
29. Cox, E.; Laessig, K. FDA approval of bedaquiline--the benefit-risk balance for drug-resistant tuberculosis. *N. Engl. J. Med.* **2014**, *371*, 689-691.
30. Matsumoto, M.; Hashizume, H.; Tomishige, T.; Kawasaki, M.; Tsubouchi, H.; Sasaki, H.; Shimokawa, Y.; Komatsu, M. OPC-67683, a nitro-dihydro-imidazooxazole derivative with promising action against tuberculosis in vitro and in mice. *PLoS Med.* **2006**, *3*, e466.
31. Ryan, N. J.; Lo, J. H. Delamanid: first global approval. *Drugs* **2014**, *74*, 1041-1045.
32. Stover, C. K.; Warrener, P.; VanDevanter, D. R.; Sherman, D. R.; Arain, T. M.; Langhorne, M. H.; Anderson, S. W.; Towell, J. A.; Yuan, Y.; McMurray, D. N.; Kreiswirth, B. N.; Barry, C. E.; Baker, W. R. A small-molecule nitroimidazopyran drug candidate for the treatment of tuberculosis. *Nature* **2000**, *405*, 962-966.
33. Keam, S. J. Pretomanid: first approval. *Drugs* **2019**, *79*, 1797-1803.

34. Mdluli, K.; Spigelman, M. Novel targets for tuberculosis drug discovery. *Curr. Opin. Pharmacol.* **2006**, *6*, 459-467.

35. Udwadia, Z. F.; Amale, R. A.; Ajbani, K. K.; Rodrigues, C. Totally drug-resistant tuberculosis in India. *Clin. Infect. Dis.* **2012**, *54*, 579-581.

36. Field, S. K. Bedaquiline for the treatment of multidrug-resistant tuberculosis: great promise or disappointment? *Ther. Adv. Chronic. Dis.* **2015**, *6*, 170-184.

37. Li, Y.; Sun, F.; Zhang, W. Bedaquiline and delamanid in the treatment of multidrug-resistant tuberculosis: Promising but challenging. *Drug Dev. Res.* **2019**, *80*, 98-105.

38. Brown, K. A.; Ratledge, C. The effect of p-aminosalicyclic acid on iron transport and assimilation in mycobacteria. *Biochim. Biophys. Acta.* **1975**, *385*, 207-220.

39. Zheng, J.; Rubin, E. J.; Bifani, P.; Mathys, V.; Lim, V.; Au, M.; Jang, J.; Nam, J.; Dick, T.; Walker, J. R. Para-aminosalicylic acid is a prodrug targeting dihydrofolate reductase in *Mycobacterium tuberculosis*. *J. Biol. Chem.* **2013**, *288*, 23447-23456.

40. Rengarajan, J.; Sassetti, C. M.; Naroditskaya, V.; Sloutsky, A.; Bloom, B. R.; Rubin, E. J. The folate pathway is a target for resistance to the drug para-aminosalicylic acid (PAS) in mycobacteria. *Mol. Microbiol.* **2004**, *53*, 275-282.

41. Mathys, V.; Wintjens, R.; Lefevre, P.; Bertout, J.; Singhal, A.; Kiass, M.; Kurepina, N.; Wang, X. M.; Mathema, B.; Baulard, A.; Kreiswirth, B. N.; Bifani, P. Molecular genetics of para-aminosalicylic acid resistance in clinical isolates and spontaneous mutants of *Mycobacterium tuberculosis*. *Antimicrob. Agents Chemother.* **2009**, *53*, 2100-2109.

42. Hinshaw, H. C.; Feldman, W. H.; Pfuetze, K. H. Streptomycin in treatment of clinical tuberculosis. *Am. Rev. Tuberc.* **1946**, *54*, 191-203.

43. Nair, J.; Rouse, D. A.; Bai, G. H.; Morris, S. L. The rpsL gene and streptomycin resistance in single and multiple drug-resistant strains of *Mycobacterium tuberculosis*. *Mol. Microbiol.* **1993**, *10*, 521-527.

44. Johnsson, K.; King, D. S.; Schultz, P. G., Studies on the mechanism of action of isoniazid and ethionamide in the chemotherapy of tuberculosis. *J. Am. Chem. Soc.* **1995**, *117*, 5009-5010.

45. Van Soolingen, D.; de Haas, P. E.; Van Doorn, H. R.; Kuijper, E.; Rinder, H.; Borgdorff, M. W. Mutations at amino acid position 315 of the katG gene are associated with high-level resistance to isoniazid, other drug resistance, and successful transmission of *Mycobacterium tuberculosis* in the Netherlands. *J. Infect. Dis.* **2000**, *182*, 1788-1790.

46. Zhang, Y.; Wade, M. M.; Scorpio, A.; Zhang, H.; Sun, Z. Mode of action of pyrazinamide: disruption of *Mycobacterium tuberculosis* membrane transport and energetics by pyrazinoic acid. *J. Antimicrob. Chemother.* **2003**, *52*, 790-795.

47. Scorpio, A.; Zhang, Y. Mutations in pncA, a gene encoding pyrazinamidase/nicotinamidase, cause resistance to the antituberculous drug pyrazinamide in tubercle bacillus. *Nat. Med.* **1996**, *2*, 662-667.

48. Takayama, K.; Kilburn, J. O. Inhibition of synthesis of arabinogalactan by ethambutol in *Mycobacterium smegmatis*. *Antimicrob. Agents Chemother.* **1989**, *33*, 1493-1499.

49. Telenti, A.; Philipp, W. J.; Sreevatsan, S.; Bernasconi, C.; Stockbauer, K. E.; Wieles, B.; Musser, J. M.; Jacobs, W. R., Jr. The emb operon, a gene cluster of *Mycobacterium tuberculosis* involved in resistance to ethambutol. *Nat. Med.* **1997**, *3*, 567-570.

50. Wehrli, W. Rifampin: mechanisms of action and resistance. *Rev. Infect. Dis.* **1983**, *5*, S407-411.

51. Telenti, A.; Imboden, P.; Marchesi, F.; Lowrie, D.; Cole, S.; Colston, M. J.; Matter, L.; Schopfer, K.; Bodmer, T. Detection of rifampicin-resistance mutations in *Mycobacterium tuberculosis*. *Lancet* **1993**, *341*, 647-650.

52. Sacksteder, K. A.; Protopopova, M.; Barry, C. E.; Andries, K.; Nacy, C. A. Discovery and development of SQ109: a new antitubercular drug with a novel mechanism of action. *Future Microbiol.* **2012**, *7*, 823-837.

53. Lakshmanan, M.; Xavier, A. S. Bedaquiline–the first ATP synthase inhibitor against multi drug resistant tuberculosis. *J. Young Pharm.* **2013**, *5*, 112-115.

54. Ismail, N.; Ismail, N. A.; Omar, S. V.; Peters, R. P. H. In vitro study of stepwise acquisition of rv0678 and atpe mutations conferring bedaquiline resistance. *Antimicrob. Agents Chemother.* **2019**, *63*, e00292-00219.

55. Xavier, A. S.; Lakshmanan, M. Delamanid: a new armor in combating drug-resistant tuberculosis. *J. Pharmacol. Pharmacother.* **2014**, *5*, 222-224.

56. Rifat, D.; Li, S.-Y.; Ioerger, T.; Lanoix, J.-P.; Lee, J.; Bashiri, G.; Sacchettini, J.; Nuermberger, E. Mutations in Rv2983 as a novel determinant of resistance to nitroimidazole drugs in *Mycobacterium tuberculosis*. *bioRxiv* **2018**, 457754.

57. Yang, J. S.; Kim, K. J.; Choi, H.; Lee, S. H. Delamanid, bedaquiline, and linezolid minimum inhibitory concentration distributions and resistance-related gene mutations in multidrug-resistant and extensively drug-resistant tuberculosis in Korea. *Ann. Lab. Med.* **2018**, *38*, 563-568.

58. Manjunatha, U.; Boshoff, H. I.; Barry, C. E. The mechanism of action of PA-824: novel insights from transcriptional profiling. *Commun. Integr. Biol.* **2009**, *2*, 215-218.

59. Baptista, R.; Fazakerley, D. M.; Beckmann, M.; Baillie, L.; Mur, L. A. J. Untargeted metabolomics reveals a new mode of action of pretomanid (PA-824). *Sci. Rep.* **2018**, *8*, 5084.

60. Vergne, A. F.; Walz, A. J.; Miller, M. J. Iron chelators from mycobacteria (1954-1999) and potential therapeutic applications. *Nat. Prod. Rep.* **2000**, *17*, 99-116.

61. Ratledge, C. Iron, mycobacteria and tuberculosis. *Tuberculosis* **2004**, *84*, 110-130.

62. Quadri, L. E. Strategic paradigm shifts in the antimicrobial drug discovery process of the 21st century. *Infect. Disord. Drug. Targets.* **2007**, *7*, 230-237.

63. Messenger, A. J.; Barclay, R. Bacteria, iron and pathogenicity. *Biochem. Educ.* **1983**, *11*, 54-63.

64. Theil, E. C. The ferritin family of iron storage proteins. *Adv. Enzymol.* **1993**, *63*, 421-421.

65. Wally, J.; Buchanan, S. K. A structural comparison of human serum transferrin and human lactoferrin. *Biometals* **2007**, *20*, 249-262.

66. Ratledge, C.; Dover, L. G. Iron metabolism in pathogenic bacteria. *Annu. Rev. Microbiol.* **2000**, *54*, 881-941.

67. Quadri, L. E. Assembly of aryl-capped siderophores by modular peptide synthetases and polyketide synthases. *Mol. Microbiol.* **2000**, *37*, 1-12.

68. Miethke, M.; Marahiel, M. A. Siderophore-based iron acquisition and pathogen control. *Microbiol. Mol. Biol. Rev.* **2007**, *71*, 413-451.

69. Snow, G. A. Mycobactins: iron-chelating growth factors from mycobacteria. *Bacteriol. Rev.* **1970**, *34*, 99-125.

70. De Voss, J. J.; Rutter, K.; Schroeder, B. G.; Barry, C. E., 3rd, Iron acquisition and metabolism by mycobacteria. *J. Bacteriol.* **1999**, *181*, 4443-4451.

71. Ratledge, C.; Patel, P. V.; Mundy, J. Iron transport in *Mycobacterium smegmatis*: the location of mycobactin by electron microscopy. *J. Gen. Microbiol.* **1982**, *128*, 1559-1565.

72. Adilakshmi, T.; Ayling, P. D.; Ratledge, C. Mutational analysis of a role for salicylic acid in iron metabolism of *Mycobacterium smegmatis*. *J. Bacteriol.* **2000**, *182*, 264-271.

73. Quadri, L. E., Iron Uptake by *Mycobacterium tuberculosis*. In Handbook of Tuberculosis; Kaufmann, S.H.E., Rubin, E., Britton, W.J., Helden, P, Eds.; John Wiley & Sons, Inc., **2008**, 91-110.

74. Quadri, L. E. Biosynthesis of mycobacterial lipids by polyketide synthases and beyond. *Crit. Rev. Biochem. Mol. Biol.* **2014**, *49*, 179-211.

75. Patel, K.; Butala, S.; Khan, T.; Suvarna, V.; Sherje, A.; Dravyakar, B. Mycobacterial siderophore: a review on chemistry and biology of siderophore and its potential as a target for tuberculosis. *Eur. J. Med. Chem.* **2018**, *157*, 783-790.

76. Lane, S. J.; Marshall, P. S.; Upton, R. J.; Ratledge, C.; Ewing, M. Novel extracellular mycobactins, the carboxymycobactins from *Mycobacterium avium*. *Tetrahedron Lett.* **1995**, *36*, 4129-4132.

77. Ratledge, C.; Ewing, M. The occurrence of carboxymycobactin, the siderophore of pathogenic mycobacteria, as a second extracellular siderophore in *Mycobacterium smegmatis*. *Microbiology* **1996**, *142*, 2207-2212.

78. Lane, S. J.; Marshall, P. S.; Upton, R. J.; Ratledge, C. Isolation and characterization of carboxymycobactins as the second extracellular siderophores in *Mycobacterium smegmatis*. *Biometals* **1998**, *11*, 13-20.

79. Harrington, J. M.; Park, H.; Ying, Y.; Hong, J.; Crumbliss, A. L. Characterization of Fe(III) sequestration by an analog of the cytotoxic siderophore brasilibactin A: implications for the iron transport mechanism in mycobacteria. *Metallomics* **2011**, *3*, 464-471.

80. Sharman, G. J.; Williams, D. H.; Ewing, D. F.; Ratledge, C. Isolation, purification and structure of exochelin MS, the extracellular siderophore from *Mycobacterium smegmatis*. *Biochem. J.* **1995**, *305*, 187-196.

81. Sharman, G. J.; Williams, D. H.; Ewing, D. F.; Ratledge, C. Determination of the structure of exochelin MN, the extracellular siderophore from *Mycobacterium neoaurum*. *Chem. Biol.* **1995**, *2*, 553-561.

82. Dhungana, S.; Ratledge, C.; Crumbliss, A. L. Iron chelation properties of an extracellular siderophore exochelin MS. *Inorg. Chem.* **2004**, *43*, 6274-6283.

83. Trias, J.; Jarlier, V.; Benz, R. Porins in the cell wall of mycobacteria. *Science* **1992**, *258*, 1479-1481.

84. Trias, J.; Benz, R. Permeability of the cell wall of *Mycobacterium smegmatis*. *Mol. Microbiol.* **1994**, *14*, 283-290.

85. Calder, K. M.; Horwitz, M. A. Identification of iron-regulated proteins of *Mycobacterium tuberculosis*and cloning of tandem genes encoding a low iron-induced protein and a metal transporting ATPase with similarities to two-component metal transport systems. *Microb. Pathog.* **1998**, *24*, 133-143.

86. Rodriguez, G. M.; Smith, I. Identification of an ABC transporter required for iron acquisition and virulence in *Mycobacterium tuberculosis*. *J. Bacteriol.* **2006**, *188*, 424-430.

87. Stephenson, M. C.; Ratledge, C. Iron transport in mycobacterium smegmatis: uptake of iron from Ferriexochelin. *J. Gen. Microbiol.* **1979**, *110*, 193-202.

88. Fiss, E. H.; Yu, S.; Jacobs, W. R., Jr. Identification of genes involved in the sequestration of iron in mycobacteria: the ferric exochelin biosynthetic and uptake pathways. *Mol. Microbiol.* **1994**, *14*, 557-569.

89. Snow, G.; White, A. Chemical and biological properties of mycobactins isolated from various mycobacteria. *Biochem. J.* **1969**, *115*, 1031-1045.

90. Maurer, P. J.; Miller, M. J. Total synthesis of a mycobactin: mycobactin S2. *J. Am. Chem. Soc.* **1983**, *105*, 240-245.

91. Hu, J.; Miller, M. J. Total synthesis of a mycobactin s, a siderophore and growth promoter ofmycobacterium smegmatis, and determination of its growth inhibitory activity against *Mycobacterium tuberculosis*. *J. Am. Chem. Soc.* **1997**, *119*, 3462-3468.

92. Poreddy, A. R.; Schall, O. F.; Marshall, G. R.; Ratledge, C.; Slomczynska, U. Corrigendum to ‘Solid-phase synthesis of methyl carboxymycobactin T 7 and analogues as potential antimycobacterial agents. *Bioorg. Med. Chem. Lett.* **2003**, *13*, 3879-3879.

93. Quadri, L. E.; Sello, J.; Keating, T. A.; Weinreb, P. H.; Walsh, C. T. Identification of a *Mycobacterium tuberculosis* gene cluster encoding the biosynthetic enzymes for assembly of the virulence-conferring siderophore mycobactin. *Chem. Biol.* **1998**, *5*, 631-645.

94. Chavadi, S. S.; Stirrett, K. L.; Edupuganti, U. R.; Vergnolle, O.; Sadhanandan, G.; Marchiano, E.; Martin, C.; Qiu, W. G.; Soll, C. E.; Quadri, L. E. Mutational and phylogenetic analyses of the mycobacterial mbt gene cluster. *J. Bacteriol.* **2011**, *193*, 5905-5913.

95. McMahon, M. D.; Rush, J. S.; Thomas, M. G. Analyses of MbtB, MbtE, and MbtF suggest revisions to the mycobactin biosynthesis pathway in *Mycobacterium tuberculosis*. *J. Bacteriol.* **2012**, *194*, 2809-2818.

96. Schmitt, M. P.; Predich, M.; Doukhan, L.; Smith, I.; Holmes, R. K. Characterization of an iron-dependent regulatory protein (IdeR) of *Mycobacterium tuberculosis* as a functional homolog of the diphtheria toxin repressor (DtxR) from Corynebacterium diphtheriae. *Infect. Immun.* **1995**, *63*, 4284-4289.

97. Krithika, R.; Marathe, U.; Saxena, P.; Ansari, M. Z.; Mohanty, D.; Gokhale, R. S. A genetic locus required for iron acquisition in *Mycobacterium tuberculosis*. *Proc. Natl. Acad. Sci. U. S. A.* **2006**, *103*, 2069-2074.

98. Macheroux, P.; Schmid, J.; Amrhein, N.; Schaller, A. A unique reaction in a common pathway: mechanism and function of chorismate synthase in the shikimate pathway. *Planta* **1999**, *207*, 325-334.

99. Parish, T.; Stoker, N. G. The common aromatic amino acid biosynthesis pathway is essential in *Mycobacterium tuberculosis*. *Microbiology* **2002**, *148*, 3069-3077.

100. Kerbarh, O.; Ciulli, A.; Howard, N. I.; Abell, C. Salicylate biosynthesis: overexpression, purification, and characterization of Irp9, a bifunctional salicylate synthase from *Yersinia enterocolitica*. *J. Bacteriol.* **2005**, *187*, 5061-5066.

101. Harrison, A. J.; Ramsay, R. J.; Baker, E. N.; Lott, J. S. Crystallization and preliminary X-ray crystallographic analysis of MbtI, a protein essential for siderophore biosynthesis in *Mycobacterium tuberculosis*. *Acta Crystallogr. Sect. F Struct. Biol. Cryst. Commun.* **2005**, *61*, 121-123.

102. Harrison, A. J.; Yu, M.; Gårdenborg, T.; Middleditch, M.; Ramsay, R. J.; Baker, E. N.; Lott, J. S. The structure of MbtI from *Mycobacterium tuberculosis*, the first enzyme in the biosynthesis of the siderophore mycobactin, reveals it to be a salicylate synthase. *J. Bacteriol.* **2006**, *188*, 6081-6091.

103. Vergnolle, O.; Xu, H.; Tufariello, J. M.; Favrot, L.; Malek, A. A.; Jacobs, W. R., Jr.; Blanchard, J. S. Post-translational acetylation of MbtA modulates mycobacterial siderophore biosynthesis. *J. Biol. Chem.* **2016**, *291*, 22315-22326.

104. Moody, D. B.; Young, D. C.; Cheng, T. Y.; Rosat, J. P.; Roura-Mir, C.; O'Connor, P. B.; Zajonc, D. M.; Walz, A.; Miller, M. J.; Levery, S. B.; Wilson, I. A.; Costello, C. E.; Brenner, M. B. T cell activation by lipopeptide antigens. *Science* **2004**, *303*, 527-531.

105. Card, G. L.; Peterson, N. A.; Smith, C. A.; Rupp, B.; Schick, B. M.; Baker, E. N. The crystal structure of Rv1347c, a putative antibiotic resistance protein from *Mycobacterium tuberculosis*, reveals a GCN5-related fold and suggests an alternative function in siderophore biosynthesis. *J. Biol. Chem.* **2005**, *280*, 13978-13986.

106. Lambalot, R. H.; Gehring, A. M.; Flugel, R. S.; Zuber, P.; LaCelle, M.; Marahiel, M. A.; Reid, R.; Khosla, C.; Walsh, C. T. A new enzyme superfamily—the phosphopantetheinyl transferases. *Chem. Biol.* **1996**, *3*, 923-936.

107. De Voss, J. J.; Rutter, K.; Schroeder, B. G.; Su, H.; Zhu, Y.; Barry, C. E., 3rd, The salicylate-derived mycobactin siderophores of *Mycobacterium tuberculosis* are essential for growth in macrophages. *Proc. Natl. Acad. Sci. U. S. A.* **2000**, *97*, 1252-1257.

108. Bythrow, G. V.; Mohandas, P.; Guney, T.; Standke, L. C.; Germain, G. A.; Lu, X.; Ji, C.; Levendosky, K.; Chavadi, S. S.; Tan, D. S. Kinetic analyses of the siderophore biosynthesis inhibitor salicyl-AMS and analogues as MbtA inhibitors and antimycobacterial agents. *Biochemistry* **2018**, *58*, 833-847.

109. P Duckworth, B.; M Nelson, K.; C Aldrich, C. Adenylating enzymes in *Mycobacterium tuberculosis* as drug targets. *Curr. Top. Med. Chem.* **2012**, *12*, 766-796.

110. Zwahlen, J.; Kolappan, S.; Zhou, R.; Kisker, C.; Tonge, P. J. Structure and mechanism of MbtI, the salicylate synthase from *Mycobacterium tuberculosis*. *Biochemistry* **2007**, *46*, 954-964.

111. Walsh, C. T.; Liu, J.; Rusnak, F.; Sakaitani, M. Molecular studies on enzymes in chorismate metabolism and the enterobactin biosynthetic pathway. *Chem. Rev.* **1990**, *90*, 1105-1129.

112. Dosselaere, F.; Vanderleyden, J. A metabolic node in action: chorismate-utilizing enzymes in microorganisms. *Crit. Rev. Microbiol.* **2001**, *27*, 75-131.

113. Kerbarh, O.; Bulloch, E. M.; Payne, R. J.; Sahr, T.; Rebeille, F.; Abell, C. Mechanistic and inhibition studies of chorismate-utilizing enzymes. *Biochem. Soc. Trans.* **2005**, *33*, 763-766.

114. Kozlowski, M. C.; Bartlett, P. A. Synthesis of a potential transition-state analog inhibitor of isochorismate synthase. *J. Am. Chem. Soc.* **1991**, *113*, 5897-5898.

115. Manos-Turvey, A.; Bulloch, E. M.; Rutledge, P. J.; Baker, E. N.; Lott, J. S.; Payne, R. J. Inhibition studies of *Mycobacterium tuberculosis* salicylate synthase (MbtI). *ChemMedChem* **2010**, *5*, 1067-1079.

116. Manos-Turvey, A.; Cergol, K. M.; Salam, N. K.; Bulloch, E. M.; Chi, G.; Pang, A.; Britton, W. J.; West, N. P.; Baker, E. N.; Lott, J. S.; Payne, R. J. Synthesis and evaluation

of *M. tuberculosis* salicylate synthase (MbtI) inhibitors designed to probe plasticity in the active site. *Org. Biomol. Chem.* **2012**, *10*, 9223-9236.

117. Liu, Z.; Liu, F.; Aldrich, C. C. Stereocontrolled synthesis of a potential transition-state inhibitor of the salicylate synthase MbtI from *Mycobacterium tuberculosis*. *J. Org. Chem.* **2015**, *80*, 6545-6552.

118. Zhang, X. K.; Liu, F.; Fiers, W. D.; Sun, W. M.; Guo, J.; Liu, Z.; Aldrich, C. C. Synthesis of transition-state inhibitors of chorismate utilizing enzymes from bromobenzene cis-1,2-dihydrodiol. *J. Org. Chem.* **2017**, *82*, 3432-3440.

119. Pini, E.; Poli, G.; Tuccinardi, T.; Chiarelli, L. R.; Mori, M.; Gelain, A.; Costantino, L.; Villa, S.; Meneghetti, F.; Barlocco, D. New chromane-based derivatives as inhibitors of *Mycobacterium tuberculosis* salicylate synthase (MbtI): preliminary biological evaluation and molecular modeling studies. *Molecules* **2018**, *23*, 1506.

120. Vasan, M.; Neres, J.; Williams, J.; Wilson, D. J.; Teitelbaum, A. M.; Remmel, R. P.; Aldrich, C. C. Inhibitors of the salicylate synthase (MbtI) from *Mycobacterium tuberculosis* discovered by high-throughput screening. *ChemMedChem* **2010**, *5*, 2079-2087.

121. Chiarelli, L. R.; Mori, M.; Barlocco, D.; Beretta, G.; Gelain, A.; Pini, E.; Porcino, M.; Mori, G.; Stelitano, G.; Costantino, L. Discovery and development of novel salicylate synthase (MbtI) furanic inhibitors as antitubercular agents. *Eur. J. Med. Chem.* **2018**, *155*, 754-763.

122. Chi, G.; Manos-Turvey, A.; O'Connor, P. D.; Johnston, J. M.; Evans, G. L.; Baker, E. N.; Payne, R. J.; Lott, J. S.; Bulloch, E. M. Implications of binding mode and active site flexibility for inhibitor potency against the salicylate synthase from *Mycobacterium tuberculosis*. *Biochemistry* **2012**, *51*, 4868-4879.

123. Chiarelli, L. R.; Mori, M.; Beretta, G.; Gelain, A.; Pini, E.; Sammartino, J. C.; Stelitano, G.; Barlocco, D.; Costantino, L.; Lapillo, M. New insight into structure-activity of furan-

based salicylate synthase (MbtI) inhibitors as potential antitubercular agents. *J. Enzyme Inhib. Med. Chem.* **2019**, *34*, 823-828.

124. Mori, M.; Stelitano, G.; Gelain, A.; Pini, E.; Chiarelli, L. R.; Sammartino, J. C.; Poli, G.; Tuccinardi, T.; Beretta, G.; Porta, A.; Bellinzoni, M.; Villa, S.; Meneghetti, F. Shedding X-ray light on the role of magnesium in the activity of *Mycobacterium tuberculosis* salicylate synthase (MbtI) for drug design. *J. Med. Chem.* **2020**, *63*, 7066-7080.

125. Ferguson, L.; Wells, G.; Bhakta, S.; Johnson, J.; Guzman, J.; Parish, T.; Prentice, R. A.; Brucoli, F. Integrated target-based and phenotypic screening approaches for the identification of anti-tubercular agents that bind to the mycobacterial adenylating enzyme MbtA. *ChemMedChem* **2019**, *14*, 1735-1741.

126. Ferreras, J. A.; Ryu, J. S.; Di Lello, F.; Tan, D. S.; Quadri, L. E. Small-molecule inhibition of siderophore biosynthesis in *Mycobacterium tuberculosis* and *Yersinia pestis*. *Nat. Chem. Biol.* **2005**, *1*, 29-32.

127. Lun, S.; Guo, H.; Adamson, J.; Cisar, J. S.; Davis, T. D.; Chavadi, S. S.; Warren, J. D.; Quadri, L. E.; Tan, D. S.; Bishai, W. R. Pharmacokinetic and in vivo efficacy studies of the mycobactin biosynthesis inhibitor salicyl-AMS in mice. *Antimicrob. Agents Chemother.* **2013**, *57*, 5138-5140.

128. Somu, R. V.; Boshoff, H.; Qiao, C.; Bennett, E. M.; Barry, C. E.; Aldrich, C. C. Rationally designed nucleoside antibiotics that inhibit siderophore biosynthesis of mycobacterium tuberculosis. *J. Med. Chem.* **2006**, *49*, 31-34.

129. Vannada, J.; Bennett, E. M.; Wilson, D. J.; Boshoff, H. I.; Barry, C. E.; Aldrich, C. C., Design, synthesis, and biological evaluation of β-ketosulfonamide adenylation inhibitors as potential antitubercular agents. *Org. Lett.* **2006**, *8*, 4707-4710.

130. Miethke, M.; Bisseret, P.; Beckering, C. L.; Vignard, D.; Eustache, J.; Marahiel, M. A. Inhibition of aryl acid adenylation domains involved in bacterial siderophore synthesis. *FEBS J.* **2006**, *273*, 409-419.

131. Qiao, C.; Gupte, A.; Boshoff, H. I.; Wilson, D. J.; Bennett, E. M.; Somu, R. V.; Barry, C. E.; Aldrich, C. C. 5 '-O-[(N-acyl) sulfamoyl] adenosines as antitubercular agents that inhibit MbtA: an adenylation enzyme required for siderophore biosynthesis of the mycobactins. *J. Med. Chem.* **2007**, *50*, 6080-6094.

132. Engelhart, C. A.; Aldrich, C. C. Synthesis of chromone, quinolone, and benzoxazinone sulfonamide nucleosides as conformationally constrained inhibitors of adenylating enzymes required for siderophore biosynthesis. *J. Org. Chem.* **2013**, *78*, 7470-7481.

133. Veber, D. F.; Johnson, S. R.; Cheng, H.-Y.; Smith, B. R.; Ward, K. W.; Kopple, K. D. Molecular properties that influence the oral bioavailability of drug candidates. *J. Med. Chem.* **2002**, *45*, 2615-2623.

134. Nelson, K. M.; Viswanathan, K.; Dawadi, S.; Duckworth, B. P.; Boshoff, H. I.; Barry, C. E., 3rd; Aldrich, C. C. Synthesis and pharmacokinetic evaluation of siderophore biosynthesis inhibitors for *Mycobacterium tuberculosis*. *J. Med. Chem.* **2015**, *58*, 5459-5475.

135. Dawadi, S.; Boshoff, H. I.; Park, S. W.; Schnappinger, D.; Aldrich, C. C. Conformationally constrained cinnolinone nucleoside analogues as siderophore biosynthesis inhibitors for tuberculosis. *ACS Med. Chem. Lett.* **2018**, *9*, 386-391.

136. Somu, R. V.; Wilson, D. J.; Bennett, E. M.; Boshoff, H. I.; Celia, L.; Beck, B. J.; Barry, C. E.; Aldrich, C. C. Antitubercular nucleosides that inhibit siderophore biosynthesis: SAR of the glycosyl domain. *J. Med. Chem.* **2006**, *49*, 7623-7635.

137. Dawadi, S.; Viswanathan, K.; Boshoff, H. I.; Barry, C. E., 3rd; Aldrich, C. C. Investigation and conformational analysis of fluorinated nucleoside antibiotics targeting siderophore biosynthesis. *J. Org. Chem.* **2015**, *80*, 4835-4850.

138. Dawadi, S.; Kawamura, S.; Rubenstein, A.; Remmel, R.; Aldrich, C. C. Synthesis and pharmacological evaluation of nucleoside prodrugs designed to target siderophore biosynthesis in *Mycobacterium tuberculosis*. *Bioorg. Med. Chem.* **2016**, *24*, 1314-1321.

139. Neres, J.; Labello, N. P.; Somu, R. V.; Boshoff, H. I.; Wilson, D. J.; Vannada, J.; Chen, L.; Barry, C. E., 3rd; Bennett, E. M.; Aldrich, C. C. Inhibition of siderophore biosynthesis in *Mycobacterium tuberculosis* with nucleoside bisubstrate analogues: structure-activity relationships of the nucleobase domain of 5'-O-[N-(salicyl)sulfamoyl]adenosine. *J. Med. Chem.* **2008**, *51*, 5349-5370.

140. Krajczyk, A.; Zeidler, J.; Januszczyk, P.; Dawadi, S.; Boshoff, H. I.; Barry III, C. E.; Ostrowski, T.; Aldrich, C. C., 2-Aryl-8-aza-3-deazaadenosine analogues of 5′-O-[N-(salicyl) sulfamoyl] adenosine: nucleoside antibiotics that block siderophore biosynthesis in *Mycobacterium tuberculosis*. *Bioorg. Med. Chem.* **2016**, *24*, 3133-3143.

141. Vergnolle, O.; Xu, H.; Blanchard, J. S. Mechanism and regulation of mycobactin fatty acyl-AMP ligase FadD33. *J. Biol. Chem.* **2013**, *288*, 28116-28125.

142. Guillet, V.; Galandrin, S.; Maveyraud, L.; Ladevèze, S.; Mariaule, V.; Bon, C.; Eynard, N.; Daffé, M.; Marrakchi, H.; Mourey, L. Insight into structure-function relationships and inhibition of the fatty Acyl-AMP ligase (FadD32) orthologs from mycobacteria. *J. Biol. Chem.* **2016**, *291*, 7973-7989.

143. Crosa, J. H.; Walsh, C. T. Genetics and assembly line enzymology of siderophore biosynthesis in bacteria. *Microbiol. Mol. Biol. Rev.* **2002**, *66*, 223-249.

144. Keating, T. A.; Walsh, C. T. Initiation, elongation, and termination strategies in polyketide and polypeptide antibiotic biosynthesis. *Curr. Opin. Chem. Biol.* **1999**, *3*, 598-606.

145. Walsh, C. T.; Gehring, A. M.; Weinreb, P. H.; Quadri, L. E.; Flugel, R. S. Post-translational modification of polyketide and nonribosomal peptide synthases. *Curr. Opin. Chem. Biol.* **1997**, *1*, 309-315.

146. Duckworth, B. P.; Aldrich, C. C. Development of a high-throughput fluorescence polarization assay for the discovery of phosphopantetheinyl transferase inhibitors. *Anal. Biochem.* **2010**, *403*, 13-19.

147. Vickery, C. R.; Kosa, N. M.; Casavant, E. P.; Duan, S.; Noel, J. P.; Burkart, M. D. Structure, biochemistry, and inhibition of essential 4'-phosphopantetheinyl transferases from two species of Mycobacteria. *ACS Chem. Biol.* **2014**, *9*, 1939-1944.

148. Rohilla, A.; Khare, G.; Tyagi, A. K. A combination of docking and cheminformatics approaches for the identification of inhibitors against 4′ phosphopantetheinyl transferase of *Mycobacterium tuberculosis*. *RSC Adv.* **2018**, *8*, 328-341.

149. Grunewald, J.; Klock, H. E.; Cellitti, S. E.; Bursulaya, B.; McMullan, D.; Jones, D. H.; Chiu, H.-P.; Wang, X.; Patterson, P.; Zhou, H. Efficient preparation of site-specific antibody–drug conjugates using phosphopantetheinyl transferases. *Bioconjug. Chem.* **2015**, *26*, 2554-2562.

150. Stirrett, K. L.; Ferreras, J. A.; Jayaprakash, V.; Sinha, B. N.; Ren, T.; Quadri, L. E. Small molecules with structural similarities to siderophores as novel antimicrobials against *Mycobacterium tuberculosis* and *Yersinia pestis*. *Bioorg. Med. Chem. Lett.* **2008**, *18*, 2662-2668.

151. Ferreras, J. A.; Gupta, A.; Amin, N. D.; Basu, A.; Sinha, B. N.; Worgall, S.; Jayaprakash, V.; Quadri, L. E. Chemical scaffolds with structural similarities to

siderophores of nonribosomal peptide–polyketide origin as novel antimicrobials against *Mycobacterium tuberculosis* and *Yersinia pestis*. *Bioorg. Med. Chem. Lett.* **2011**, *21*, 6533-6537.

152. Moraski, G. C.; Chang, M.; Villegas-Estrada, A.; Franzblau, S. G.; Mollmann, U.; Miller, M. J. Structure-activity relationship of new anti-tuberculosis agents derived from oxazoline and oxazole benzyl esters. *Eur. J. Med. Chem.* **2010**, *45*, 1703-1716.

153. Moraski, G. C.; Franzblau, S. G.; Miller, M. J. Utiliztion of the suzuki coupling to enhance the antituberculosis activity of aryl oxazoles. *Heterocycles* **2010**, *80*, 977-988.

154. Veerepalli, P.; Vijayakumar, V.; Sarveswari, S. Siderophore inhibitors: synthesis and antimycobacterial evaluation of certain chromeno [4, 3-d] benzimidazo [1, 2-a] pyrimidines. *J. Pharm. Res.* **2012**, *5*, 1027-1033.

155. Pokrovskaya, V.; Baasov, T. Dual-acting hybrid antibiotics: a promising strategy to combat bacterial resistance. *Expert Opin. Drug Discov.* **2010**, *5*, 883-902.

156. Schalk, I. J. A trojan-horse strategy including a bacterial suicide action for the efficient use of a specific Gram-positive antibiotic on Gram-negative bacteria. *J. Med. Chem.* **2018**, *61*, 3842–3844.

157. Miller, M. J.; Walz, A. J.; Zhu, H.; Wu, C.; Moraski, G.; Möllmann, U.; Tristani, E. M.; Crumbliss, A. L.; Ferdig, M. T.; Checkley, L. Design, synthesis, and study of a mycobactin− artemisinin conjugate that has selective and potent activity against tuberculosis and malaria. *J. Am. Chem. Soc.* **2011**, *133*, 2076-2079.

158. Juárez-Hernández, R. E.; Franzblau, S. G.; Miller, M. J. Syntheses of mycobactin analogs as potent and selective inhibitors of *Mycobacterium tuberculosis*. *Org. Biomol. Chem.* **2012**, *10*, 7584-7593.

159. Cassat, J. E.; Skaar, E. P. Iron in infection and immunity. *Cell Host Microbe.* **2013**, *13*, 509-519.

160. Skaar, E. P.; Raffatellu, M. Metals in infectious diseases and nutritional immunity. *Metallomics* **2015**, *7*, 926-928.

161. Walsh, C. T.; Chen, H.; Keating, T. A.; Hubbard, B. K.; Losey, H. C.; Luo, L.; Marshall, C. G.; Miller, D. A.; Patel, H. M. Tailoring enzymes that modify nonribosomal peptides during and after chain elongation on NRPS assembly lines. *Curr. Opin. Chem. Biol.* **2001**, *5*, 525-534.

162. Walsh, C. T. Polyketide and nonribosomal peptide antibiotics: modularity and versatility. *Science* **2004**, *303*, 1805-1810.

Table of Contents Graphic